DISCLAIMER NOTICE

THIS DOCUMENT IS THE BEST QUALITY AVAILABLE.

COPY FURNISHED CONTAINED A SIGNIFICANT NUMBER OF PAGES WHICH DO NOT REPRODUCE LEGIBLY.

OCEAN-BOTTOM SEISMOMETER DATA ANALYSIS PROGRAM

SEMI-ANNUAL TECHNICAL REPORT NO. 5

TEXAS INSTRUMENTS
INCORPORATED
SCIENCE SERVICES DIVISION

(5) 861000

ARPA Order No. 292-62
ARPA Project Code No. 8100

November 14, 1963

(21) ORIGINAL CONTAINS COLOR PLATES: ALL DDC REPRODUCTIONS WILL BE IN BLACK AND WHITE. ORIGINAL MAY BE SEEN IN DDC HEADQUARTERS.

(6) OCEAN-BOTTOM SEISMOMETER DATA COLLECTION AND ANALYSIS

(9) SEMI-ANNUAL TECHNICAL REPORT, NO. 5

~~Project Manager~~
P. J. Farrell

Telephone
Dallas, Texas
FLeetwood 7-4311
Extension 262

Contractor: Texas Instruments Incorporated
Date of Contract: 15 March 1961
Contract Expiration Date: 21 June 1964

Contract No. AF 19(604)-8368
Amount of Contract $1,547,431.00

-A-

ACKNOWLEDGMENTS

This program is supported through the Air Force Cambridge Research Laboratories as part of the Advanced Research Project Agency's Project VELA UNIFORM.

The data analysis section of this report was performed by and under the direction of Dr. William A. Schneider of Texas Instruments Incorporated Science Services Division.

The author wishes to acknowledge the contribution of the United States Coast and Geodetic Survey for providing the USC&GS Ship SURVEYOR during the collection phase in the Aleutians. Also, the Air Force Cambridge Research Laboratories' Major Robert A. Gray whose presence aboard ship and assistance in obtaining use of Government equipment and facilities contributed to the success of the program.

ABSTRACT

A total of 300 hours of ocean-bottom seismic data have been collected in areas off the California Coast and north and south of the Aleutian Chain in varying water depths to 20,000 feet.

Refraction data of Pn arrivals recorded at Adak and on the ocean bottom (from 1000-pound explosive sources in water) yield an average 8.5 Km/second velocity which may be attributed to crustal thickening in the vicinity of the Aleutian Chain.

Detailed analyses of a near-regional event recorded simultaneously on land and on the ocean bottom in the vicinity of Cape Mendocino, California, show signal-to-noise ratios on land and ocean bottom are comparable with enrichment of the high frequencies on the ocean bottom. The phases are better defined and developed on the ocean bottom than on land.

Analyses of land and ocean-bottom noise samples in the California area indicate that at the microseismic peak the ocean-bottom average noise power levels are 20 db greater than at a nearby land station. Both the land and ocean-bottom noise spectra show little variation with time for the samples investigated, and their sources appear to be distributed in azimuth.

TABLE OF CONTENTS

Section	Title	Page
	ABSTRACT	
I	INTRODUCTION	1/2
II	DATA COLLECTION	3
	A. GENERAL	3
	B. EQUIPMENT	3
	C. TIME SCHEDULE	8
	D. RESULTS	10
III	REFRACTION PROFILE	11
IV	DATA ANALYSIS	13
	A. NOISE SPECTRA	14
	B. SIGNAL EVENTS	29
	C. SUMMARY	35

LIST OF ILLUSTRATIONS

Figure	Title	Page
1.	The Ocean-Bottom Seismometer	4
2.	Seismometer Implanted on Ocean Bottom	5
3.	Rigging to Decouple Seismometer from Anchor	6
4.	The Motor Vessel WINN	7
5.	Suggested Anchor Cable Lengths	9
6.	Pn Refraction Profile	12
7.	Average Noise Power Spectra - Vertical Component	15
8.	Average Noise Power Spectra - Horizontal Component	16
9.	Average Noise Power Spectra - Horizontal Component	17
10.	Average Noise Power Spectra - Pressure Component	18
11.	Hi and Lo Gain Pressure Power Spectra for June 20	20
12.	Seismometer Recording Positions	23/24
13.	Coherence Noise Samples	26
14.	Coherence Noise Samples	27
15.	Comparison of Actual Vs. Theoretical Ocean-Bottom Layering	28
16.	Power Density Spectra, P-S Interval	31
17.	Power Density Spectra, S Interval	32
18.	Spectral Comparison - "S" Phase	34
TABLE I		29

SECTION I

INTRODUCTION

Texas Instruments Incorporated has developed an automatic marine seismic monitoring and recording device (ocean-bottom seismometer) to measure ocean-bottom seismic phenomena under Contract AF 19(604)-8368 for the Air Force Cambridge Research Laboratories as part of the Advanced Research Projects Agency's Project VELA UNIFORM.

Two prototype instruments capable of operation at depths to 10,000 feet were constructed and used in an initial data collection program. The initial program showed the need for development of advanced instrumentation models capable of operation at depths of 20,000 feet. Five advanced units were constructed and are currently being used in a data collection program involving three geographically separate and geologically different areas of the Pacific Ocean. The collection areas are off the California coast, off the Aleutian Islands, and off Hawaii. A detailed report on the plans and purposes of the present data collection and evaluation program was presented in Texas Instruments Proposal No. 105-GD63, dated March 21, 1963.

This report (Semi-Annual Technical Report No. 5) covers the work period of April 1 to October 1, 1963. During this time, three major goals were met:

1. Five advanced ocean-bottom seismometers were constructed;
2. The Pacific Ocean data collection program was started; and
3. Analysis of the collected data was begun.

The emphasis of this report is on the analysis program. Objectives are investigation of the signal-to-noise ratio on the ocean bottom relative to land, investigation of the nature of the signal arrivals on the ocean bottom relative to land, and investigation of the noise level and propagation modes on the ocean bottom relative to land.

All of the data collected to date has not been processed and analyzed. It takes approximately six to eight weeks after receipt of the tapes to make 16 mm film recordings for visual analysis and selection of samples for computer processing. Thus, this report will be concerned with a detailed analysis of the California data and summary reference to Aleutian results based on visual analysis of film recordings. The next semi-annual technical report will contain a detailed analysis of all collected data.

SECTION II

DATA COLLECTION

A. GENERAL

The ocean-bottom seismometer resembles a 10-foot, 1800-pound missile (see Figure 1). The unit is described in detail in Semi-Annual Technical Report No. 4.

In field operations the unit is lowered from a ship with a steel cable. Thirty feet above the ocean bottom, a tripping device releases it to free fall, thus attaining sufficient terminal velocity at impact to imbed the pointed nose cone into the bottom sediments deep enough to support the instrument in an almost vertical position (Figure 2). At this point a special chain-swivel-cable rigging is played out loosely on the ocean floor before a 750-pound anchor is set (see Figure 3). The ship remains at anchor over the seismometer during the 11-hour recording period after which the unit is retrieved. This technique was developed during initial testing with the prototype units. Subsequent work has proved it successful in decoupling spurious ship motion from the seismometers under normal (winds under 20 knots) conditions.

B. EQUIPMENT

The specialized handling procedures described above restricted the number of ships available. The most important requirement was the need for adequate clear deck space to mount the winch; it has a 32000-foot capacity of 3/8" wire rope and must be no closer than 60 feet to the sheave on the "A" frame for proper level-wind operation. Other considerations were seaworthiness, speed, supply capacity and accommodations. The Motor Vessel WINN, a 128-foot supply vessel, best filled these requirements in that the 96 by 25-foot clear deck area astern of the galley was adequate for the handling gear (see Figure 4).

Of the various types of wire rope available, a galvanized plow steel 19-strand type was selected on the basis of breaking strength, corrosion resistance and price. At the maximum depth of 20,000 feet, assuming 25,000 feet of cable is required to anchor the ship at this depth, the weight of the cable, anchor, unit and additional rigging is approximately 9000 lbs. The breaking strength of the 19-strand cable of 17,300 pounds allowed 8300 pounds safety factor.

In spite of these precautions one unit was lost in 11,400 feet of water off the California coast. During recovery in heavy seas, the boat was pitched by a large swell placing undue tension on the line and causing the cable to part 4,000 feet above the anchor. Inspection of the cable showed

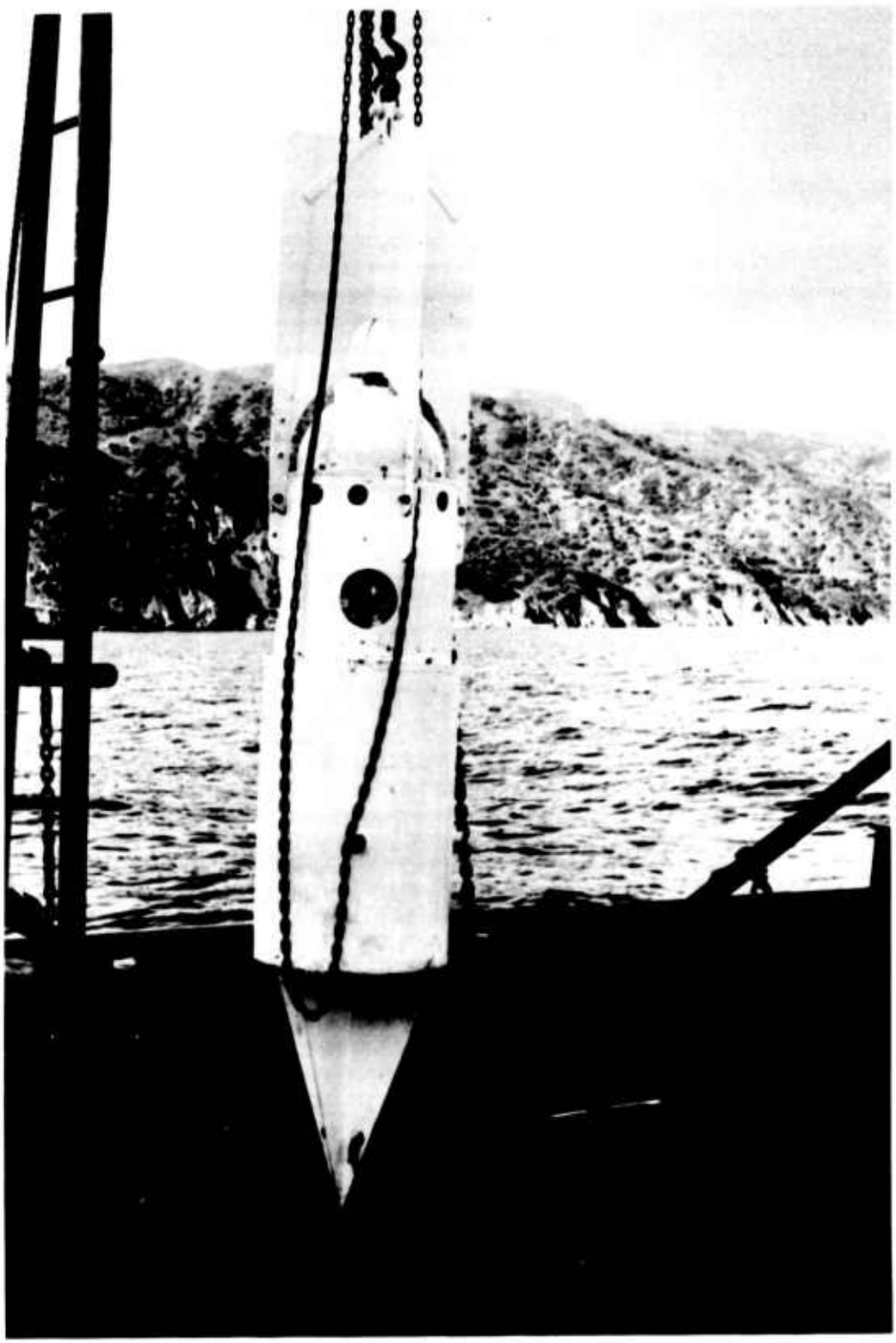

Figure 1. The Ocean-Bottom Seismometer

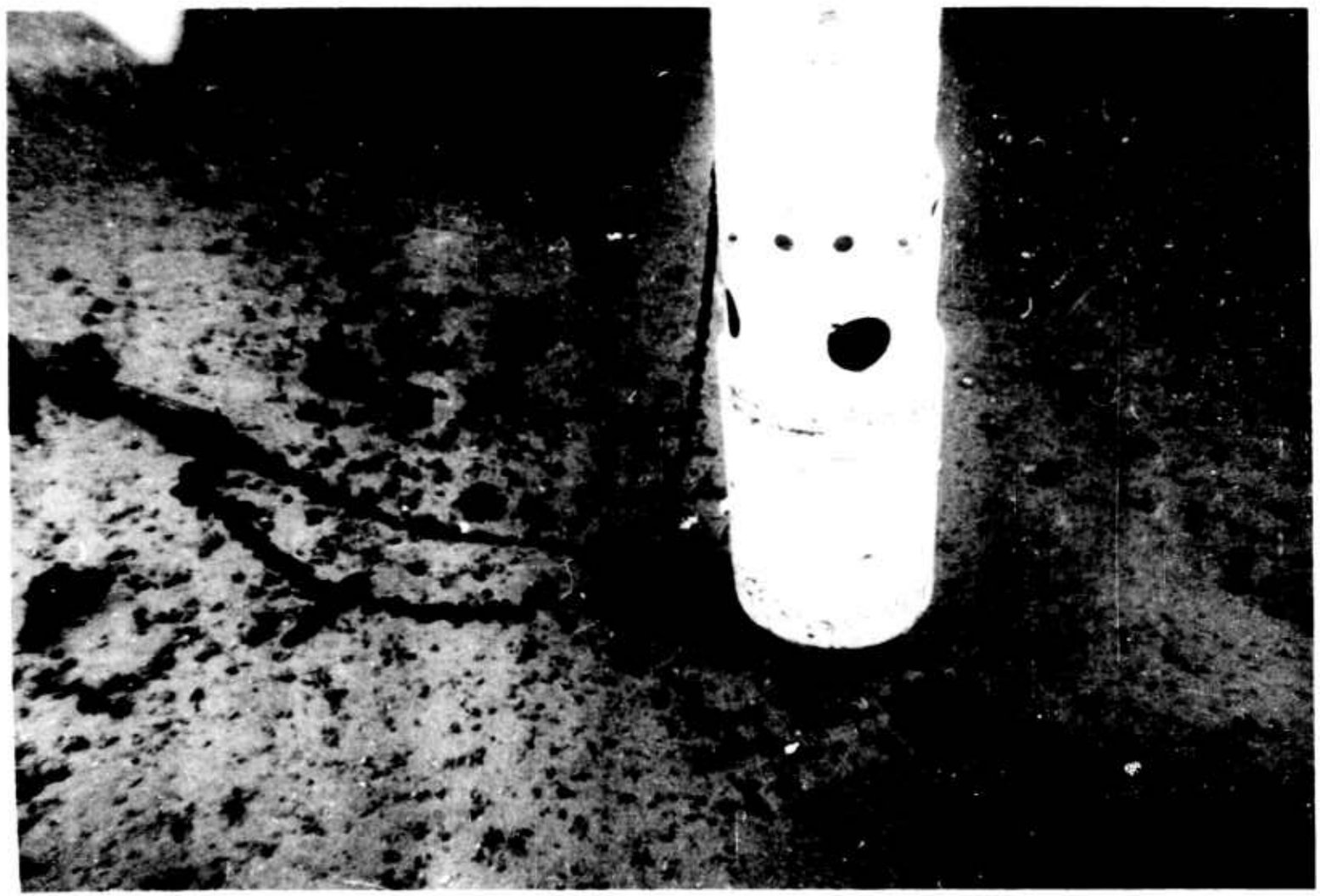

Figure 2. Seismometer Implanted on Ocean Bottom

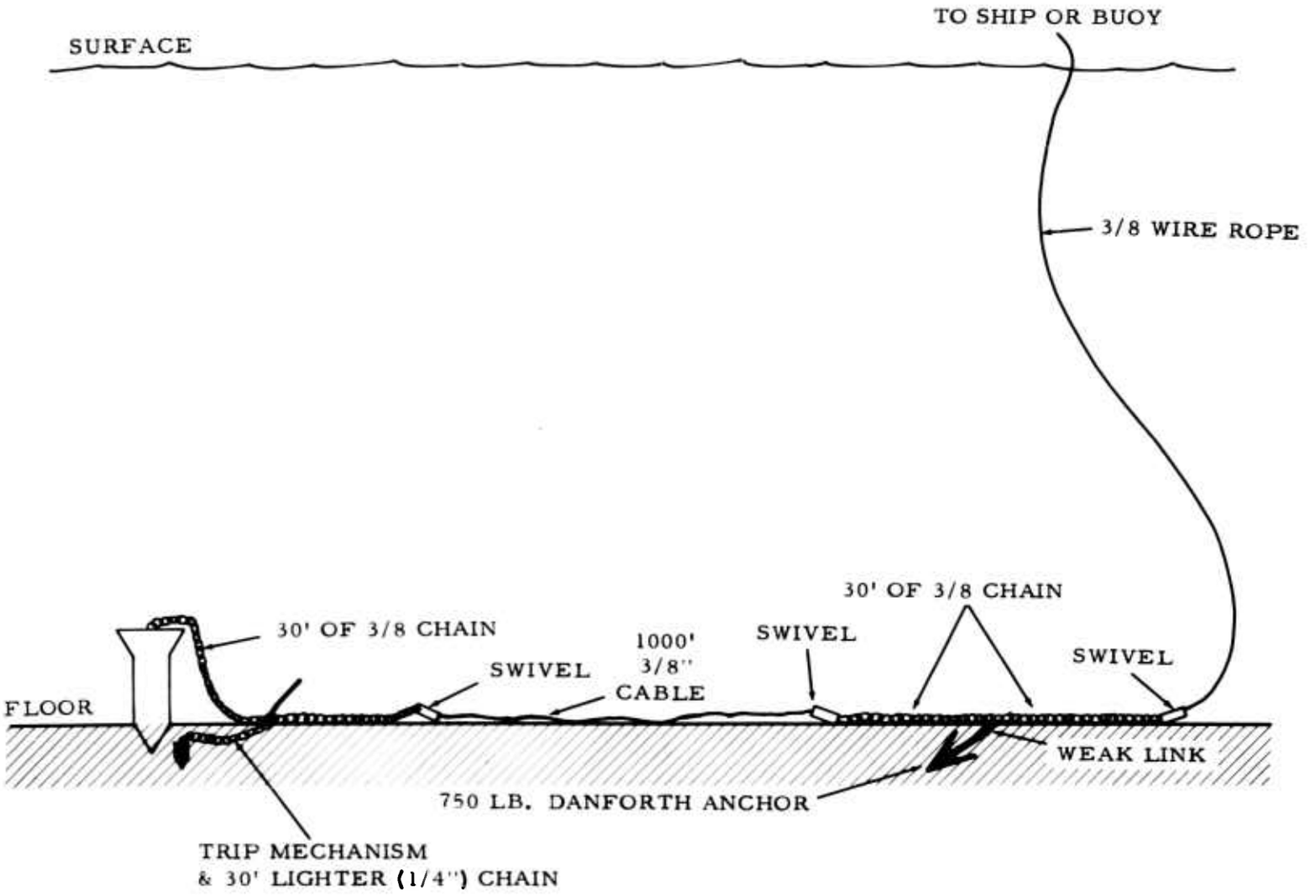

Figure 3. Rigging to Decouple Seismometer from Anchor

Figure 4. The Motor Vessel WINN
(Ship Specifications: Length 128'; Beam 31'; Engines 2-375 hp caterpillar; Power 50 KW 60 cpc AC; Fuel Capacity 38,600 gallons; Speed (loaded) 10 knots; Crew 7; Capacity 13, including 3 extra beds in trailer)

evidence of a kink 300 feet above the break leading one to suspect that excessive cable was used allowing slack to coil up on the ocean floor. Further study led to the preparation of the graph (Figure 5) showing the lengths of cable used for anchoring at various ocean depths. It appears fairly conclusive that the original assumption was correct since the amount of cable used on subsequent drops adhered closely to the lengths indicated by the graph, resulting in no additional unit losses. It should be remembered that the data given by this graph apply only to a vessel similar in wind resistance to the MV WINN.

Special Equipment. Co-operation between AFCRL and the USC&GS resulted in the acquisition of the SURVEYOR to participate in the Aleutian collection program. The SURVEYOR is a modern vessel well adapted to hydrographic and oceanic surveys and is equipped with up-to-date navigation and depth recording equipment. Its 45,000-foot capacity deep sea winch and versatile over-the-side handling gear required only the addition of a small auxiliary winch to permit handling of the unit and associated rigging.

C. TIME SCHEDULE

MV WINN

5-15 June	Prepare ship for program, install "A" frame and auxiliary winch, mount trailer, steam from Santa Barbara to Eureka, California.
16-26 July	Perform two dummy and 21 live drops in depths ranging from 1,750 to 15,000 feet.
26-30 July	Repair rigging and prepare ship for trip to Adak, Alaska.
31 July - 15 Aug.	Steam to Adak, Alaska.
16 Aug. - 11 Sept.	16 live drops south of Aleutian chain to maximum depth of 20,500 feet.
12 Sept.	Depart to Hawaiian area.

USC&GS SHIP SURVEYOR

15-17 Aug.	Prepare ship for test program north of Aleutian chain. Perform 13 live drops in water depths of 12,000 feet.

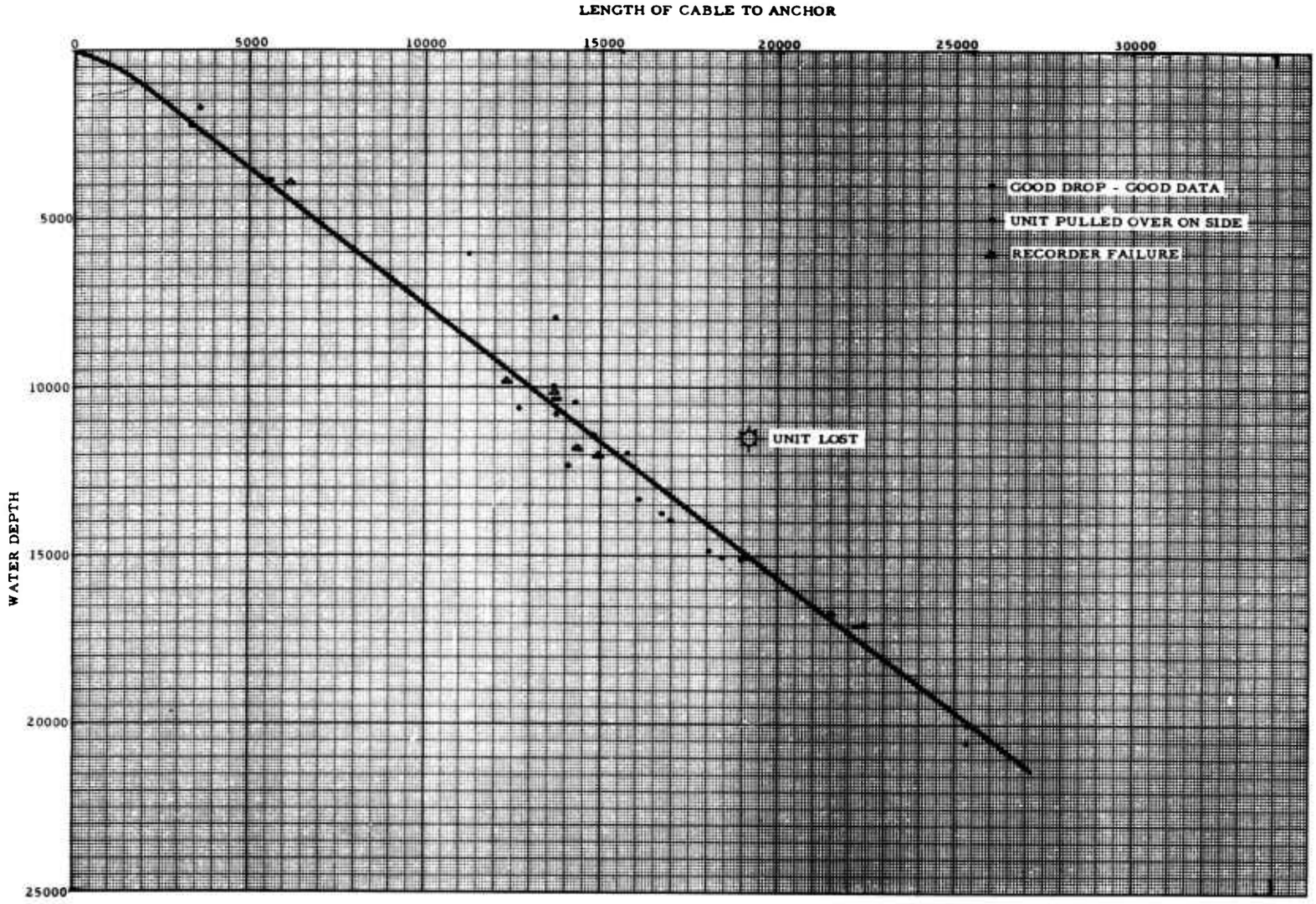

Figure 5. Suggested Anchor Cable Lengths

D. RESULTS

The results of the test program have yielded approximately 300 hours of usable ocean-bottom data leaving approximately 200 hours of data acquisition to fulfill the total proposed. Of this total, approximately 90 hours represents the California effort (versus 220 proposed), and 210 represents the Aleutian effort (versus 160 proposed). The USC&GS ship SURVEYOR contributed 110 hours of this data. Subsequent testing will continue through November to obtain the required hours in the Hawaiian area and complete the California program.

SECTION III

REFRACTION PROFILE

A nine point refraction profile showing Pn velocities to the north and south of Adak is presented in Figure 6. The points were obtained by shooting 1000-pound charges of nitramon at a depth of 300 feet below the ocean surface and recording at the land station.

The times here have been corrected to a datum of -6.2 km by replacing the water depth and underlying sediments at 1.5 and 3.0 km/second, respectively. It is apparent the velocities of 8.4 and 8.6 km/second are much higher than the expected normal of 8.1. Two possibilities exist which could cause this phenomenon; either the higher-than-normal velocities exist, or a gradual thickening of the low velocity material above the Mohorovicic discontinuity towards the arc causes a pseudo-high velocity. Compared to a velocity of 8.1 km/second, a velocity of 8.5 would result from a 2^{o} dip in this direction.

Shooting a reverse refraction profile across the chain would resolve this question but this proved to be impractical because varying weather conditions north and south of the islands prevented sufficient simultaneous ship operation.

One pair of reversed travel times across the chain (differing only by 0.2 second in 280 km) show the Pn arriving much later than would be predicted from the water-to-land Pn times. Since it is generally assumed the "Moho" deepens under the islands, the extra time may be attributed to additional travel path under this trough. Thus, using the average time delay of 4.9 seconds and a Pn velocity of 8.1 km/second, the extra travel path would be 39.7 km indicating a minimum increase in depth to the "Moho" of 14.3 km under the chain.

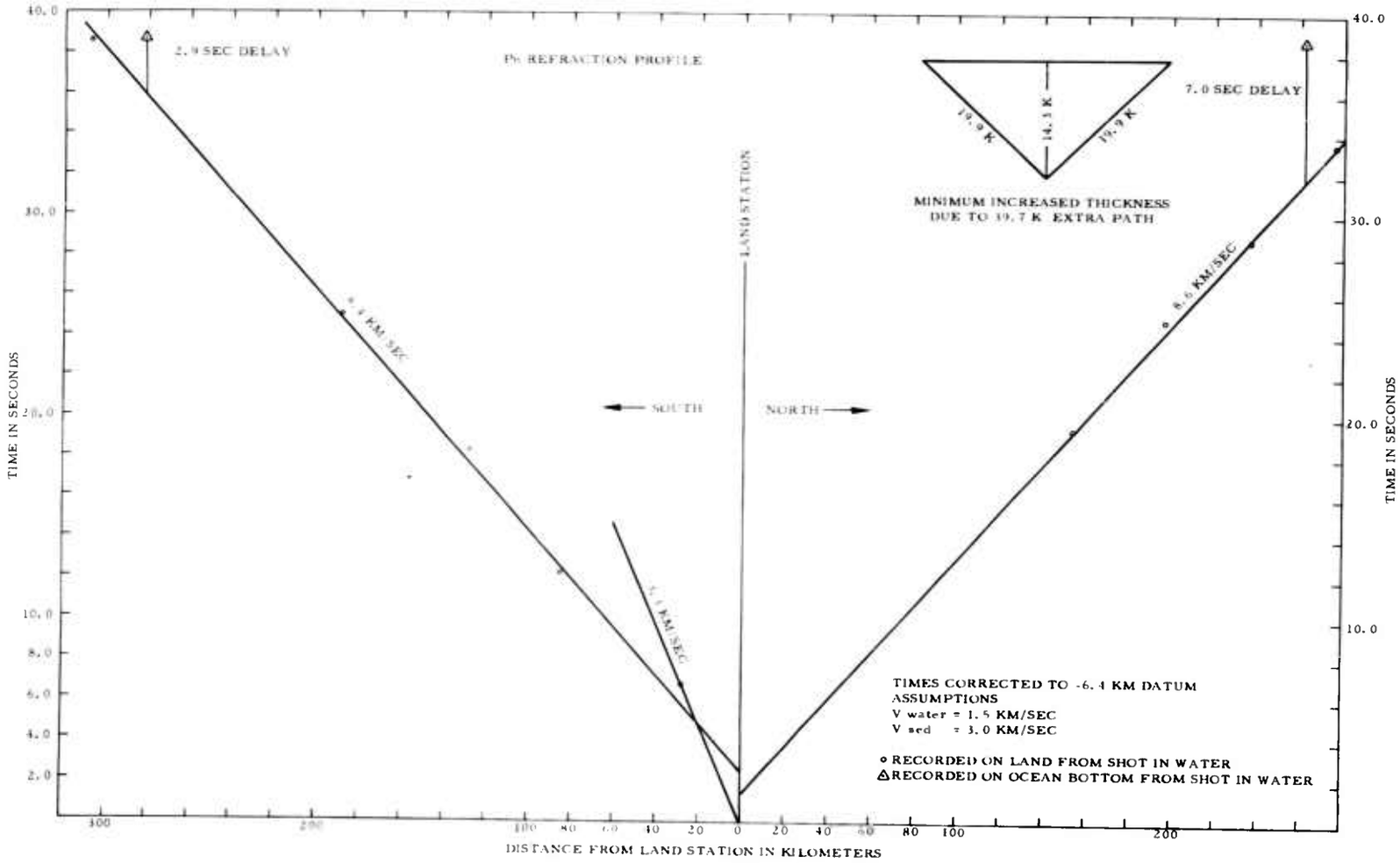

Figure 6. Pn Refraction Profile

SECTION IV

DATA ANALYSIS

Results presented in this section were obtained from analysis of the data recorded off California in the vicinity of Cape Mendocino. Data gathered in the Aleutians and Hawaiian Islands are in various stages of analysis and will be reported at a later date.

The California data were recorded simultaneously on the land and ocean bottom using identical instruments and electronics to afford a comparison of ocean bottom vs. land seismic phenomena, particulary:

1. Signal-to-noise ratios;
2. Signal characteristics (e.g., phase development, frequency content); and
3. Noise levels and propagation modes.

All of the data recorded off California were reviewed by transcribing the FM tapes to 16 mm film and viewing on a develocorder. During the 17 days on which drops were made in June and July, 1963, only two natural seismic events were recorded, and only one has been identified. This represents a total recording time on the ocean bottom of approximately 150 hours, with 195 hours on land. Of the former, about 40 per cent of the time was unusable due to a combination of problems such as recorder drive belt breakage, seismometer spring damage, and improper planting of the unit.

Receipt of only two events in the approximately 90 hours of usable ocean-bottom recording is somewhat disappointing in the seismically active California area.

Data selected to be analyzed included the identified earthquake, and noise samples from three different days in June on both the land and ocean-bottom records.

The selected samples were played back at a speed 20 times that used in recording, demodulated, fed into an analog to digital converter, and sampled at the rate of 500/second, or in real time $\frac{500}{20}$ = 25 samples/second.

Format of the digitized records is compatible with the TIAC* computer. Analog paper record playbacks were made from the digital records, and compared against playbacks made from the original FM tapes to insure fidelity of the transcription. Visual comparison revealed no loss of information or fidelity; however, spectral analysis of the digital data did uncover

*Trade Mark (Texas Instruments Automatic Computer)

60 cps pickup during transcription. This latter has subsequently been corrected for in the transcription equipment.

Power spectra were computed for the noise samples and the signal arrival on both the land and ocean-bottom records. These are presented below.

A. NOISE SPECTRA

Noise power spectra were obtained from the digital data by correlating (auto and cross) noise samples, approximately three minutes in length. The correlations were computed out to $\pm$ five seconds and fourier transformed to give spectral estimates with 0.1 cps resolution. The spectral estimates were smoothed by "hanning" (Blackman and Tukey, 1959) to reduce the correlation truncation effects. The resolution after smoothing is approximately 0.2 cps.

Spectra were computed from 0.2 cps out to 10 cps for noise samples taken on June 20, 21 and 29. Five noise samples were taken one to two hours apart from each of the three 11-hour data gathering periods. These samples were simultaneous in time between land and ocean-bottom records. Auto and cross power spectra were then computed between the pressure and three velocity components on the ocean bottom and between the three velocity components on land for each noise sample. An average spectra was then computed for each component over the five samples for each of the three days. The latter are presented in Figures 7, 8, 9 and 10 for the vertical, two horizontals, and pressure channels, respectively. It is noteworthy to mention that the individual spectra in the average did not vary significantly from the mean on a given day, indicating the time stationarity of the noise field.

Spectra presented in the above figures have not been corrected for instrument response, which rolls off -6 db per octave and -12 db per octave for the pressure and velocity components, respectively, below 1 cps. Above approximately 1 cps, the response is essentially flat, and the power density scales, $(\mu/\text{sec})^2/\text{cps}$ or $(\text{dynes/cm}^2)^2/\text{cps}$ are correct. The low frequency data, when appropriately boosted to compensate for instrument roll-off, tend toward the microseismic peak at six-second period, though this is well outside the response of the 1 cps seismometers.

The most significant difference in the noise spectra for the three days is the level difference between land and ocean bottom. At the peak, the ocean bottom is approximately 20 db noisier than land. This holds for all three components as well as all three days. In particular, the peak noise level does not change significantly over the three days analyzed, nor does it seem to be sensitive to water depth in the range of 1,700 - 10,000 feet. The noise on June 29 in 1,750 feet does, however, appear to be narrower banded in the vicinity of the peak than on the other two days; this is also evident on the land data, but to a lesser degree.

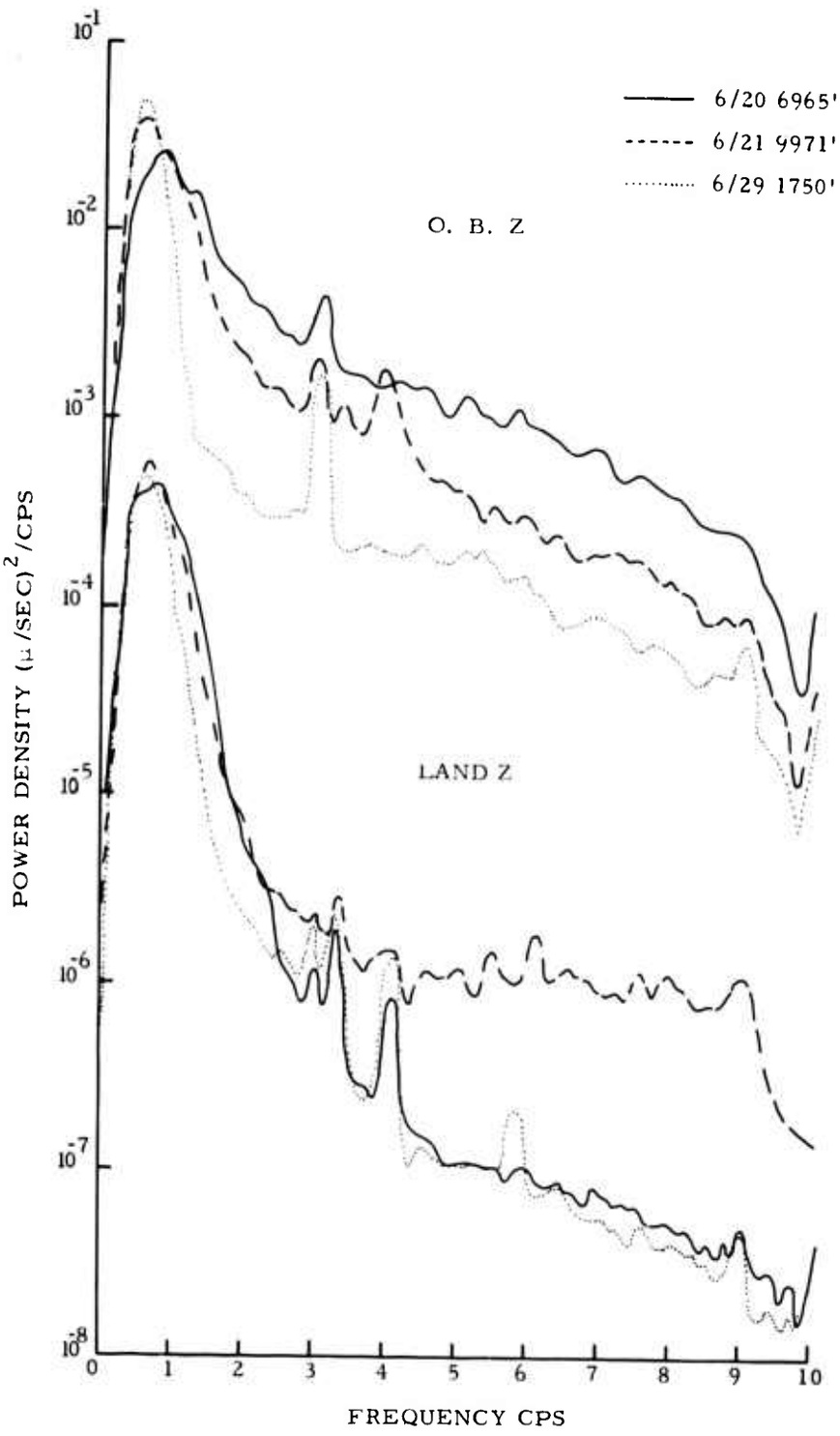

Figure 7. Average Noise Power Spectra - Vertical Component

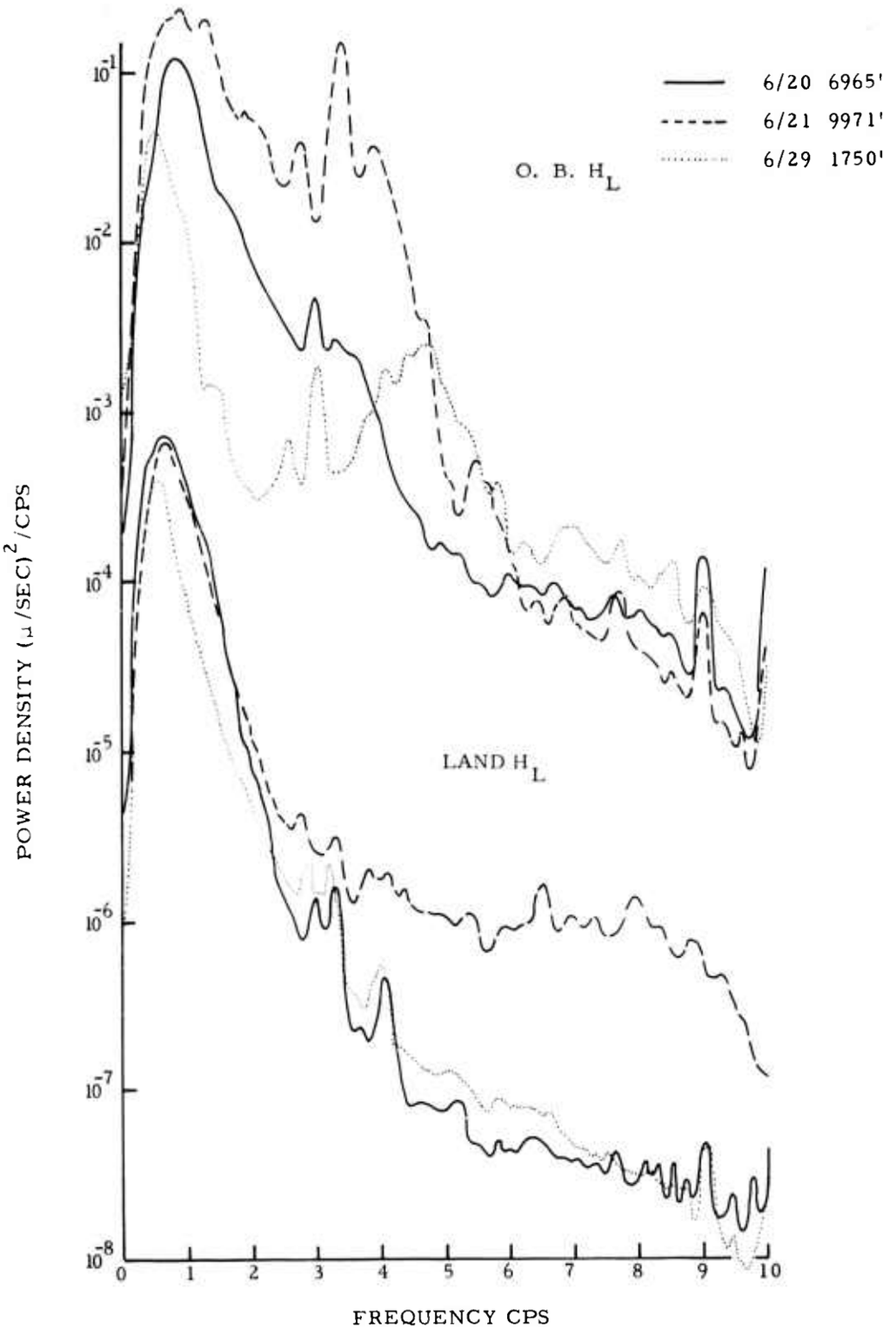

Figure 8. Average Noise Power Spectra - Horizontal Component

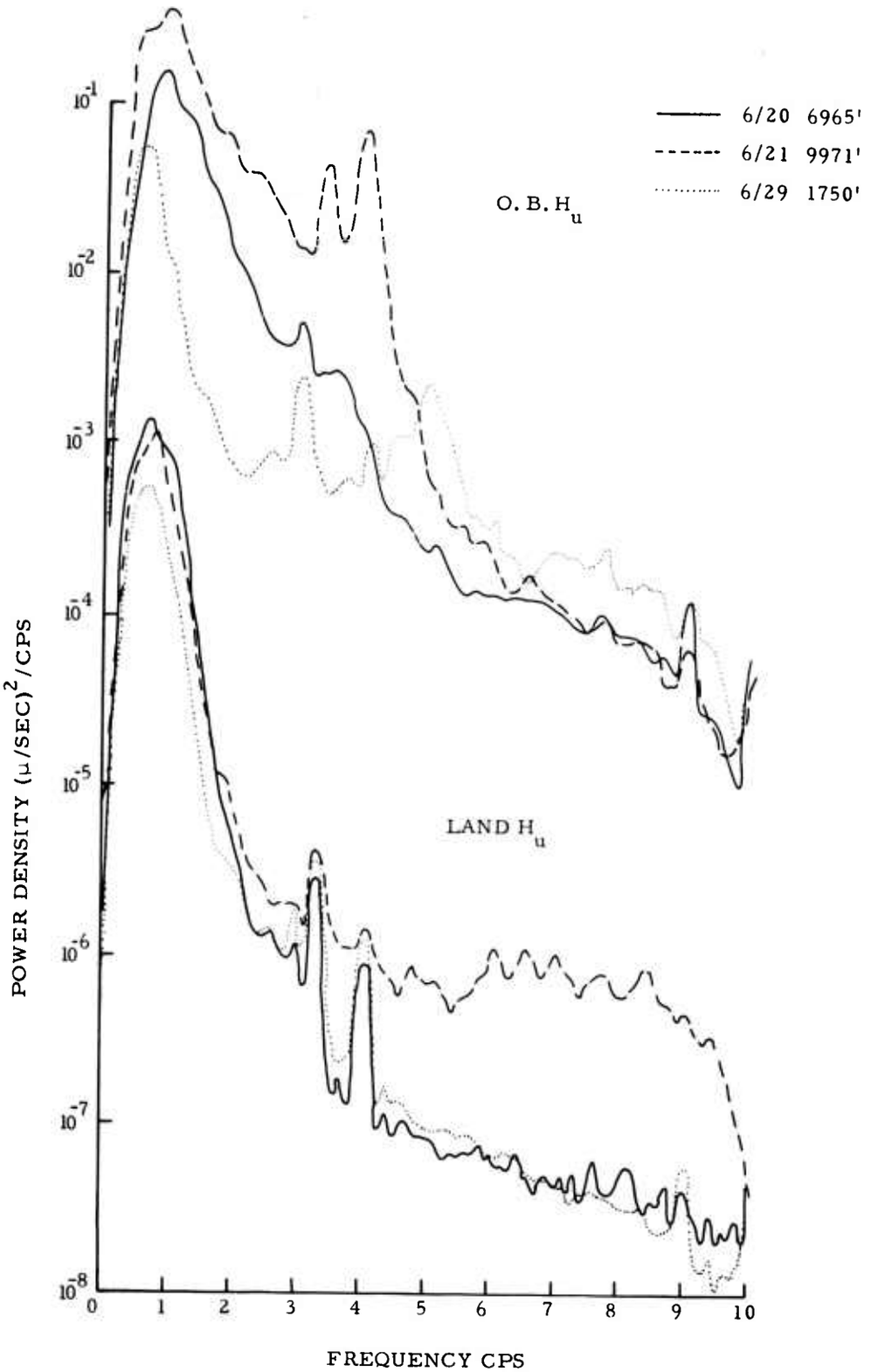

Figure 9. Average Noise Power Spectra - Horizontal Component

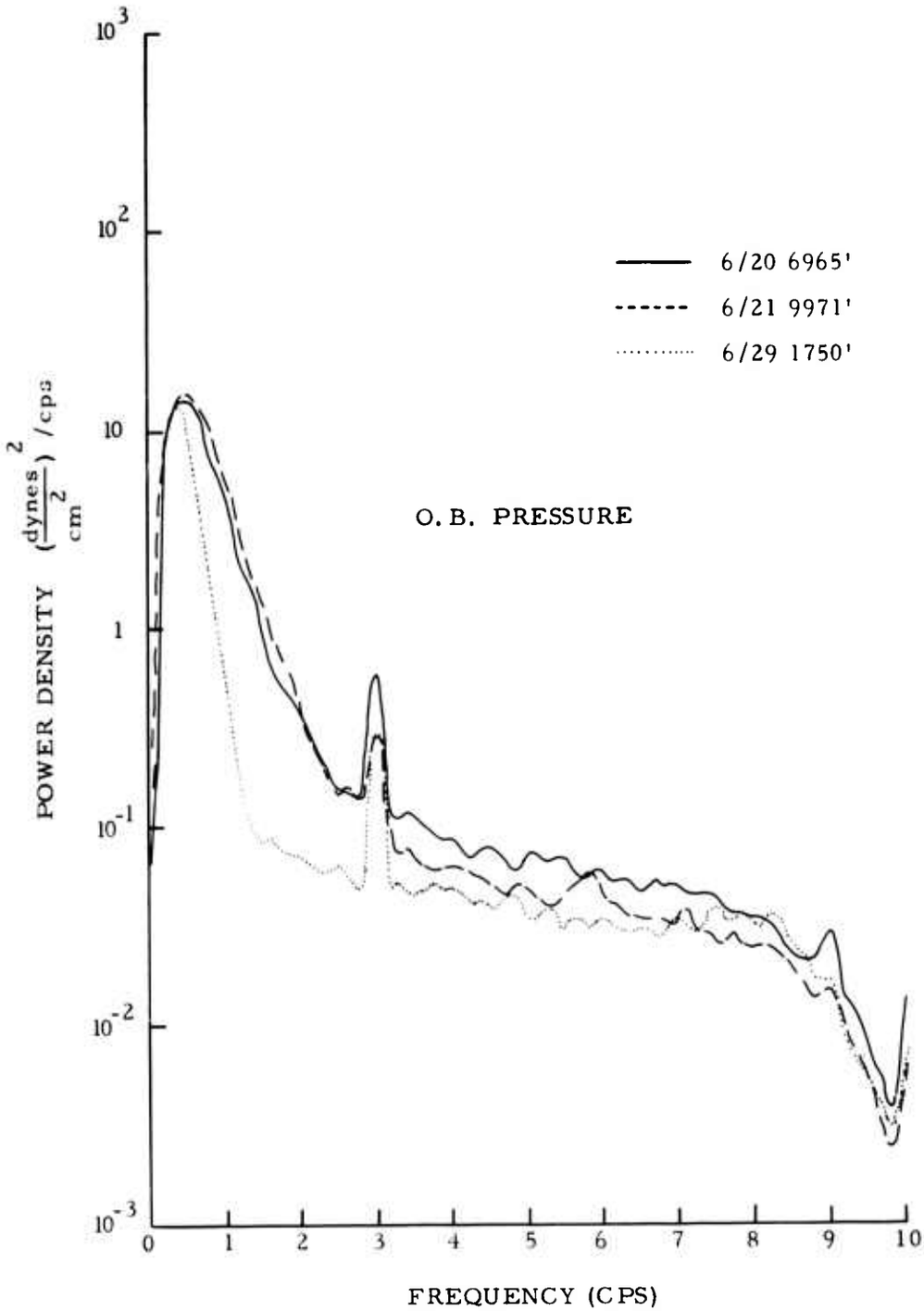

Figure 10. Average Noise Power Spectra - Pressure Component

The 60 cps pickup incurred during transcription shows up as the 3 cps "line" after frequency translation by 20 to account for transcription speed-up. This is best seen on the pressure spectra of Figure 10. The other fairly persistent lines that appear on the ocean bottom and land data at 3.4 and 4 cps are not transcription artifacts, and are believed to be seismic at the present time. Their source is unknown.

It is interesting to note that the noise field on these days appears to be isotropic in azimuth due to the equipartition of energy on the three velocity components and the lack of correlation between them discussed in a later section. This is particularly true on land where the spectra are practically indistinguishable on a given day. The relatively high land spectral level on June 21 (above 3 cps) is probably due to cultural noise (road construction was being carried on intermittently in the area). The high frequency noise background, that is, beyond the main noise peak, appears to be instrument noise level and not of seismic origin except for the June 21 land data already mentioned.

The instrument noise level for the seismometers is essentially set by the noise figure of the reactance amplifier section which is approximately 0.1 μ volt RMS equivalent input in the 1 - 10 cps band. When this level is carried through the system receiving the full 200,000 gain (the reactance amplifier is after the input attenuator so the system noise always receives full gain regardless of input attenuation) and converted to ground velocity through the sensitivity, the levels are very close to those measured above 3 - 4 cps. An assumption of slightly "colored" rather than "white" noise could account for the approximately 6 db/octave slope of the noise.

Instrument noise level for the pressure channel may be set by the reactance amplifier as above, or by thermal noise in the resistor in parallel with the transducer output whose size is a function of the attenuation setting. For the attenuations used, it appears that the thermal noise, whose mean square value is proportional to RKT, accounts for the leveling off of the pressure spectra above 2 cps (R = Resistance; K = Boltzman's Constant; T = Absolute Temperature). The drop off in the spectra above 9 cps is the result of the 9 cps aliasing filters employed in digitizing the data.

Instrument noise levels suggested here will be quantified by computing power spectra of sections of tape on which sinusoidal test signals have been recorded.

The tape noise levels can be obtained by transforming the low gain channels (30 db separation between hi and lo gain channels). Tape speed variations resulting in flutter and wow will appear on all channels at equal levels; consequently, that part of the power density in Figures 7 through 10 due to tape noise should also appear on the low gain channels equally strong, although seismic noise will be attenuated by 30 db. Figure 11 shows the hi and lo gain pressure power spectra for June 20 in $(\text{m volts})^2/\text{cps}$. Note the 60 cps pickup on both hi and lo channels at the same level. In the vicinity

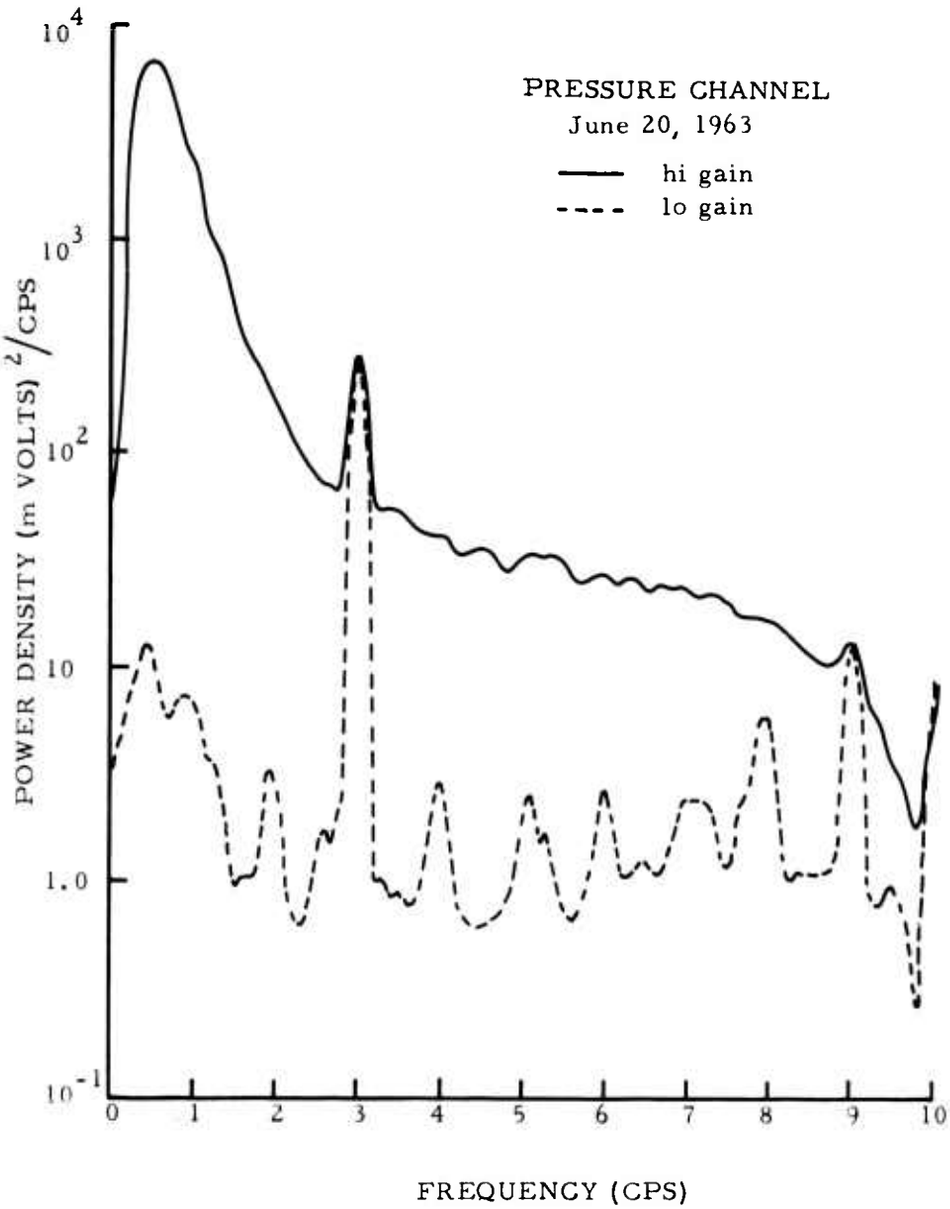

Figure 11. Hi and Lo Gain Pressure Power Spectra for June 20

of the microseismic peak at 0.5 cps the lo gain channels show this energy at 28.5 db attenuation. The remainder of the low gain data fluctuates about the 1 (m volt)^2/cps level, and remains at least 10 db below the high gain spectra out to about 8 cps. Similar findings obtain for the other channels and days analyzed. Thus we can conclude that tape noise was not a limiting factor in these data. The limits of useful seismic noise data imposed by the instrument noise levels, however, are severe. This does not reflect a serious shortcoming of the system, but rather an inefficient use of its dynamic range. The gains could have been run at a significantly higher level on the ocean bottom without endangering overmodulation of the signal arrivals on the lo gain channels. Since our charter is, however, oriented more toward study of the signal characteristics, there is a tendency to be overcautious on the gain settings.

In addition to computing power spectra for the noise data, additional processing was attempted and aimed toward understanding the noise propagation modes and spatial characteristics.

The vertical component on the ocean bottom was crosscorrelated with the vertical land component for each of the five simultaneous noise samples on the three days. The crosscorrelations were computed far enough in either direction to encompass energy propagating at 3 - 4 km/second between the two stations. Separation of the stations varied from approximately 30 - 70 km on the three drops as can be seen from Figure 12 which shows the drop locations.

The crosscorrelations were below a level deemed significant in all cases. This finding implies that the noise field does not have a strong directional character, that is, it is made up of the superposition of noise waves propagating in many directions.

This is also consistent with the crosscorrelations computed between components for a given noise sample on both the land and ocean bottom. The latter show very little correlation between the three velocity components. It can be demonstrated that for a noise field isotropic in azimuth with random phase between azimuths, the crosscorrelation or coherence between the three orthogonal velocity (or displacement) components will vanish.

The coherence was computed between channels on the ocean bottom and land for all the noise samples. The coherence is defined as:

$$\text{coh.} = \frac{\left| \phi_{12}(f) \right|}{\phi_{11}(f)\, \phi_{22}(f)}$$

where $\phi_{11}(f)$ and $\phi_{22}(f)$ are the auto power spectra of channels 1 and 2, and $\phi_{12}(f)$ is the crosspower spectrum between channels 1 and 2. The coherence function may vary between 0 and 1, and provides a measure of the statistical dependence of two time series. The coherence plots for the ocean-bottom

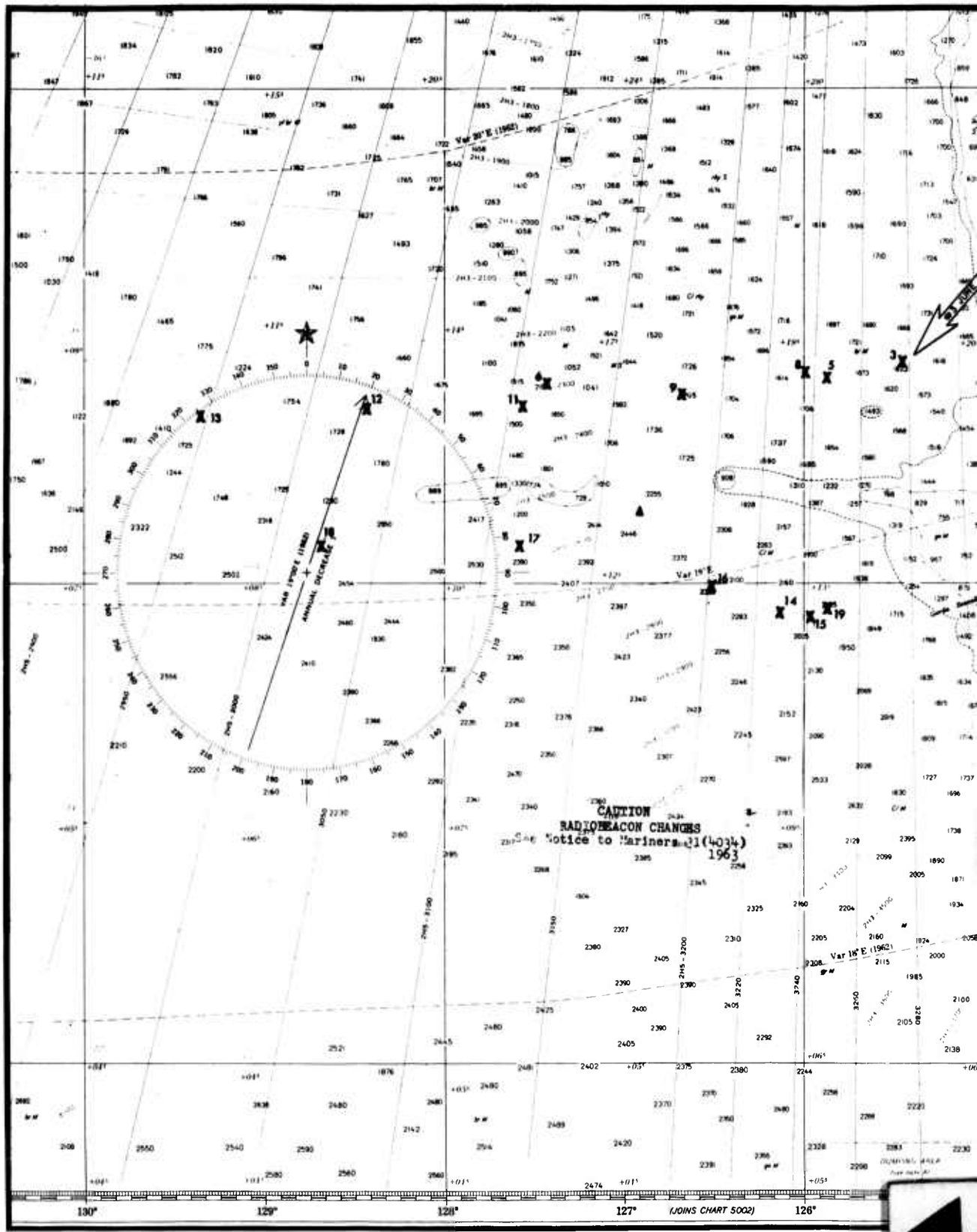
CAUTION
RADIOBEACON CHANGES
Notice to Mariners 21(4034)
1963
Var 20° E (1962)
ANNUAL DECREASE
Var 19° E (1962)
Var 18° E (1962)
130°
129°
128°
127°
(JOINS CHART 5002)
126°

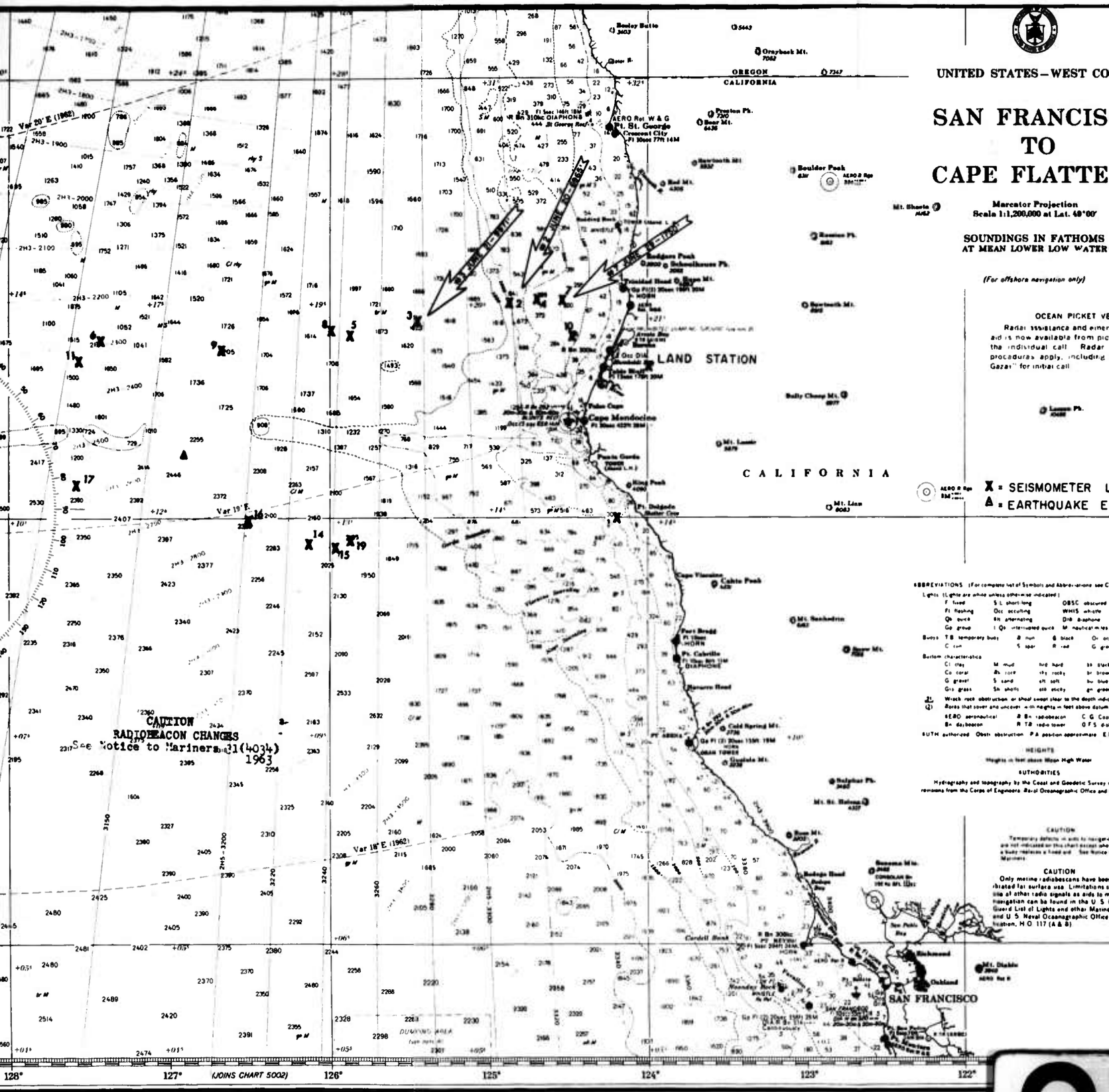

Figure 12. Seismometer Recording Po

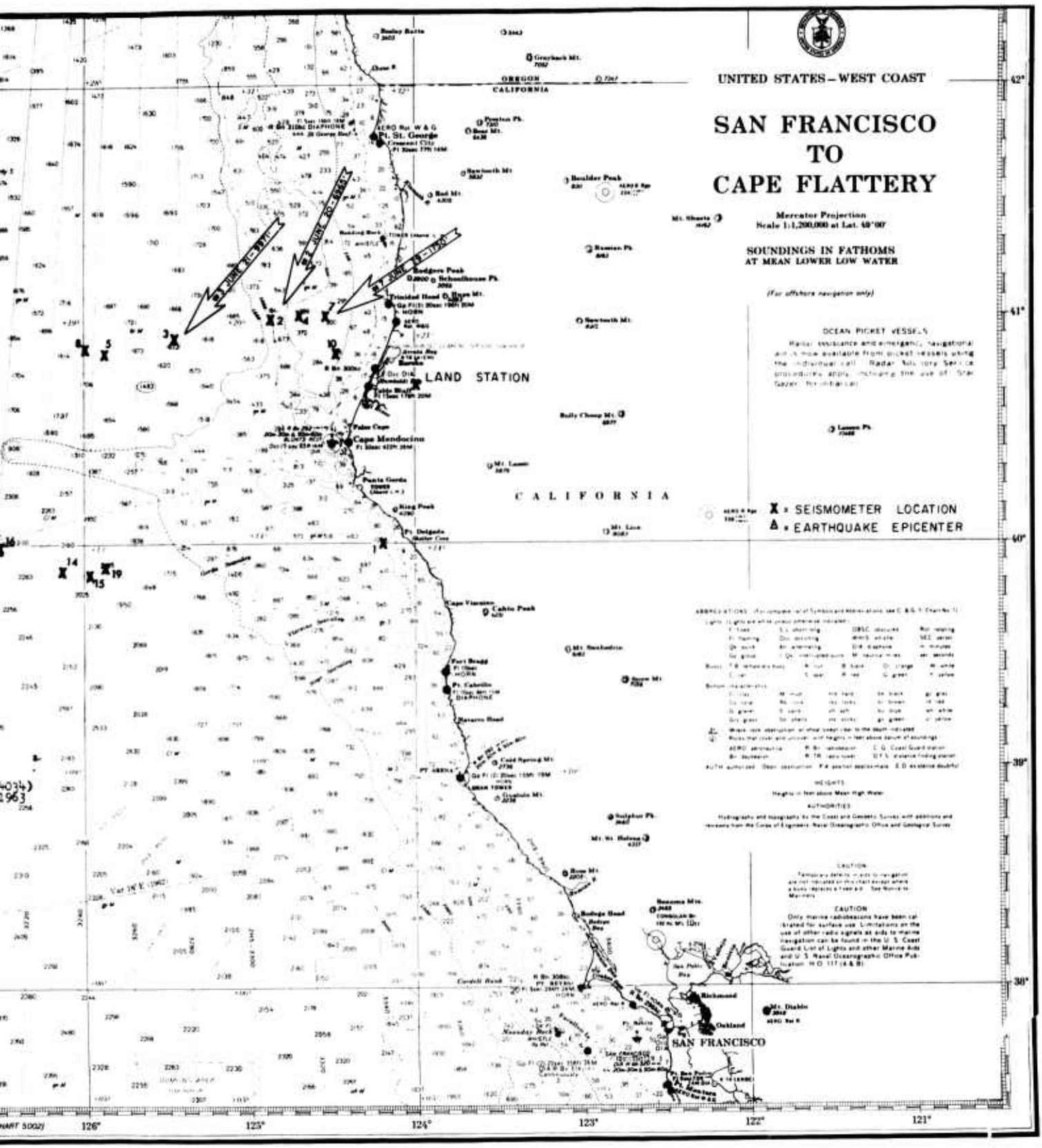

Figure 12. Seismometer Recording Positions

noise samples on June 29 are shown in Figures 13 and 14. The near perfect coherence at 3 cps is again the result of 60 cps pickup. The coherence between pressure and vertical velocity is near unity between 0.2 and 0.7 cps, the microseismic peak. For the most part, however, the coherence is low between the velocity components at the microseismic peak indicating the noise is distributed in azimuth. The drop off of the pressure-vertical velocity coherence above 1 cps is also indicative of the instrument noise level previously discussed. The latter would presumably not correlate between channels since it has independent sources. The 10 cps and sometimes 9 cps coherences on all the plots are associated with these lines in the lo gain power spectra relating to tape noise. In addition, the coherence between the two horizontal components shows broad band high coherence from about 7 - 10 cps which increases with recording time. This also is tape noise which resulted from tape speed variations that worsened with record time. It was not properly compensated on the high gain horizontal channels in transcription. Similar findings apply to the coherences computed for other days which are not presented.

In addition to the coherence estimates, pressure-vertical velocity power ratios were computed for the average noise samples on the three days. These afford in principal a means of identifying the noise modes if the bottom layering is known. Figure 15 shows the normalized power ratios plotted vs. the dimensionless quantity $\frac{Hf}{C}$, where H is the water depth, C the velocity of sound in water, and f the frequency.

Also plotted are two additional curves appropriate to the pressure-velocity power ratio for the fundamental mode, for two different oceanic models.

The latter are derived from an expression due to Bradner (1962) relating the pressure-velocity particle ratio to the phase velocity of the particular mode,

$$\frac{P}{V\rho C} = \frac{C_{i/C}}{\sqrt{\frac{C_i^2}{C^2} - 1}} \quad \tan\left(\frac{2\pi fH}{C} \sqrt{\frac{C_i^2}{C^2} - 1}\right)$$

where

P = pressure
V = vertical particle velocity
ρ = density of water
C = velocity of sound in water
C_i = phase velocity of the i^{th} mode
f^i = frequency
H = thickness of water layer

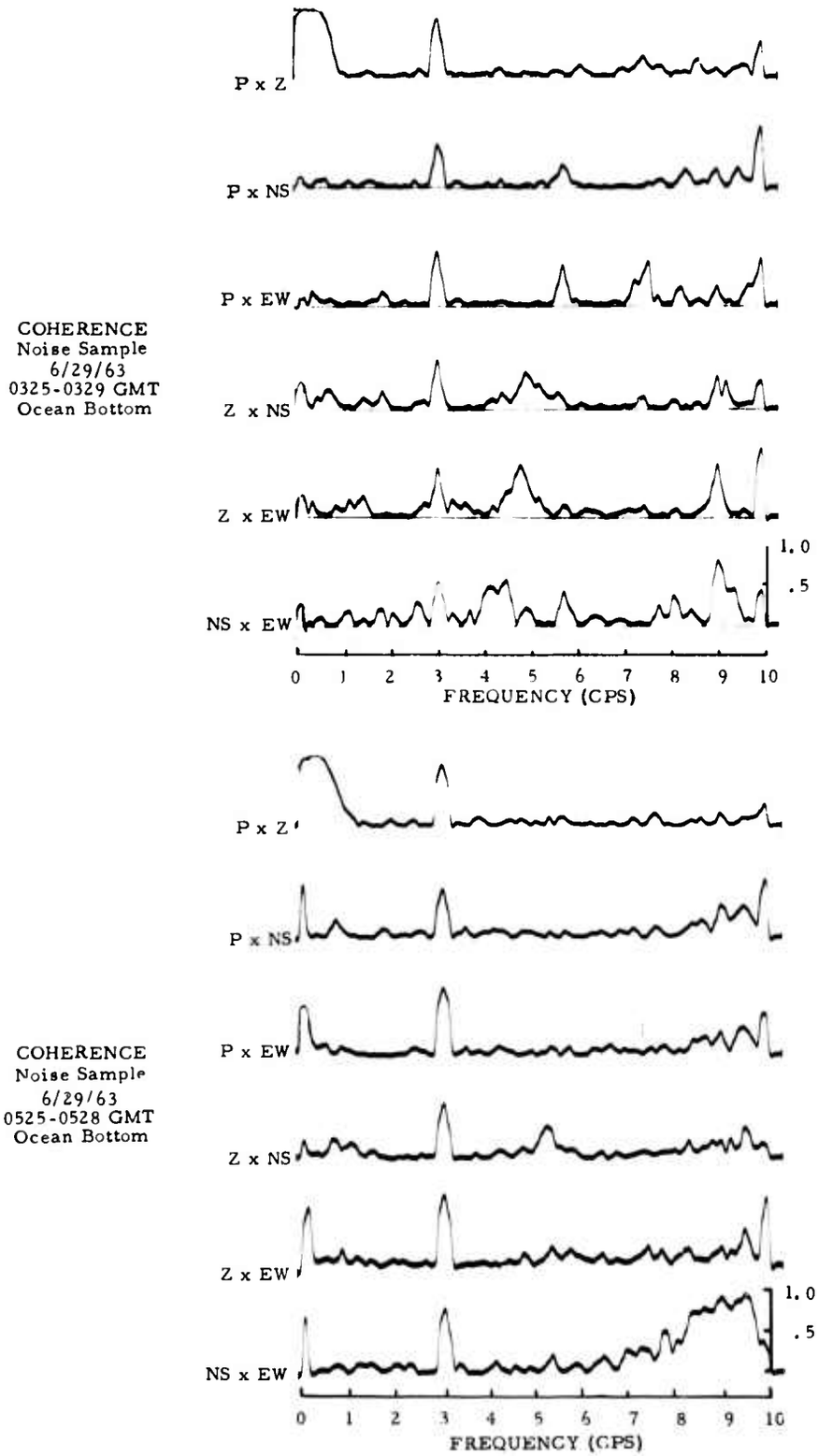

Figure 13. Coherence Noise Samples

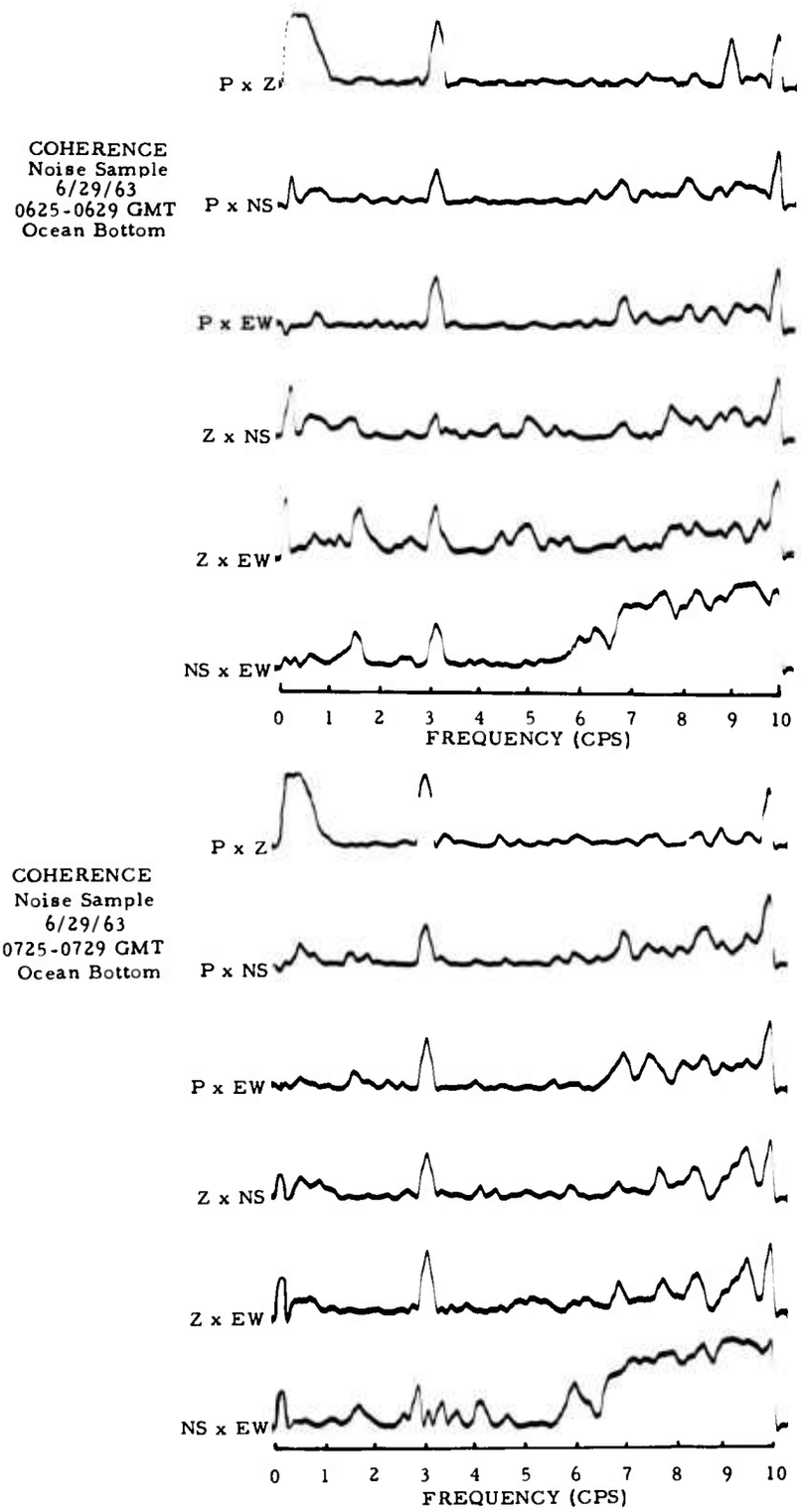

Figure 14. Coherence Noise Samples

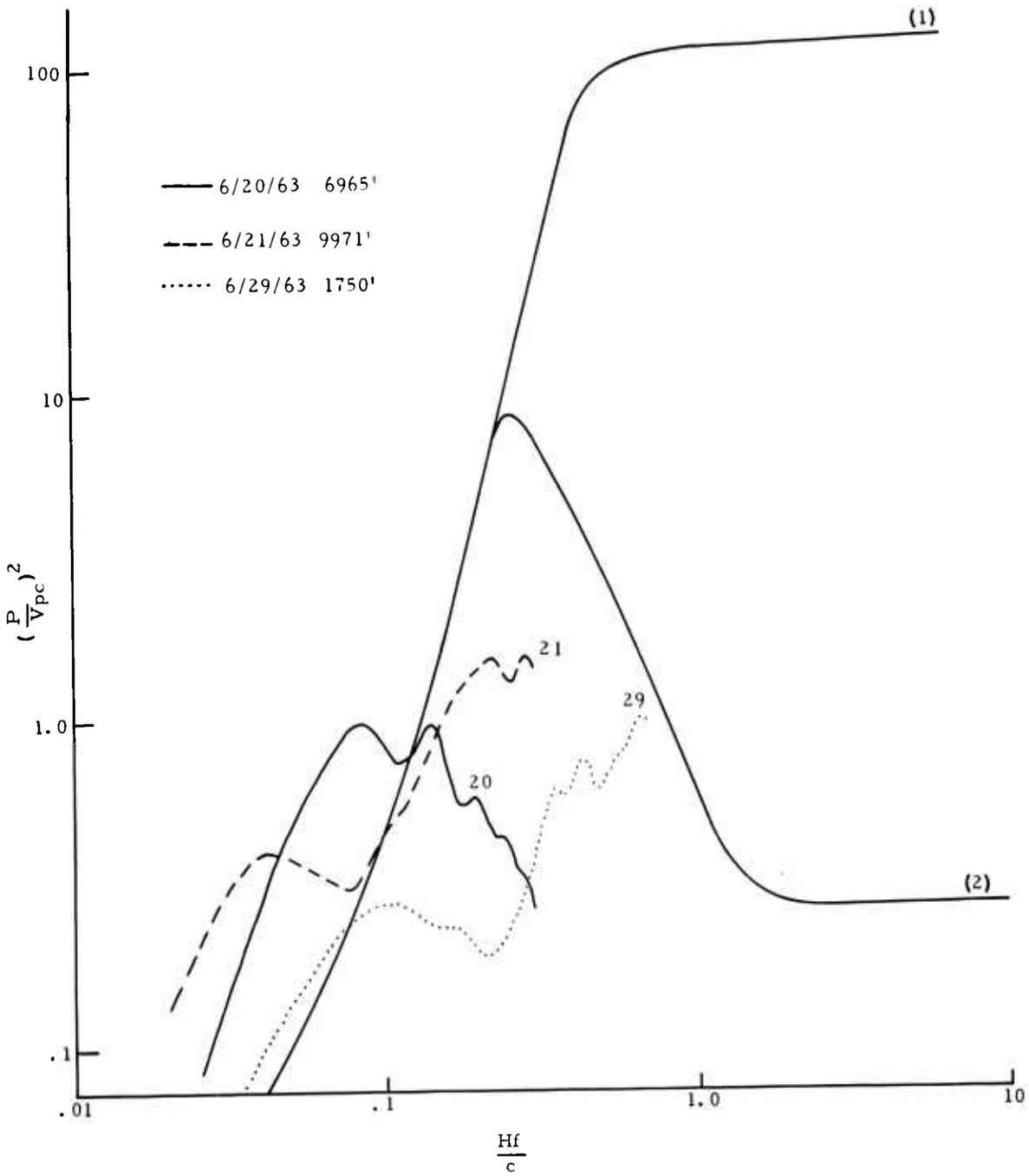

Figure 15. Comparison of Actual Vs. Theoretical Ocean-Bottom Layering

Curve (1) of Figure 15 relates to a water layer over a granitic half space, and model (2) consists of a water layer over a low velocity mud layer over an intermediate velocity lock layer over a basement half space. The layer thickness and velocities are given in Table I.

TABLE I

Model	H	ρ	V_s	V_p
1	6.0 ∞	1.03 2.58	0 3.04	1.52 5.27
2	6.0 1.0 6.0 ∞	1.03 1.03 2.75 3.09	0 1.0 3.98 4.68	1.52 1.52 6.9 8.1

The observed data do not appear to fit either model, except that the initial rise of the curves does have the correct slope. They have been carried out to the approximate instrument noise level. Models 1 and 2 are not exhaustive, of course, but they do encompass a range of likely physical situations. Curves for other models for the fundamental mode all show the same initial rise, but separate at about $\frac{Hf}{C} = 0.2$. The lack of agreement between observed and predicted pressure-vertical velocity ratios may be attributed to:

1. The noise consists of higher order modes or the superposition of several modes; and
2. The noise does not consist of horizontally propagating normal modes, but rather, leaky modes in the open organ pipe sense.

These and other possibilities will be further explored as more noise data are processed and analyzed.

B. SIGNAL EVENTS

The lone, identified signal event recorded in 1,750 feet of water off Mendocino on June 29 is shown in the fold-out for both the ocean bottom and land recordings. The ocean-bottom traces are hi gain pressure and vertical velocity, and lo gain NS and EW horizontals in that order. The land traces are all lo gain, Benioff vertical, vertical, NS, and EW horizontals, respectively. The Benioff vertical was recorded at the land station through the same ocean-bottom electronics, and is included for visual comparison purposes. Note the nearly identical traces of the Benioff and land (ocean bottom) vertical seismometers.

All the traces are filtered with a 1.8 cps cutoff on the low side. This was done to filter off the microseismic peak at 0.5 cps, and enable visual signal-to-noise ratios to be made in the pass band of the signal energy. The signal-to-noise ratios are excellent on both the land and ocean bottom records for this event in spite of the fact that the absolute noise level is approximately 20 db higher on the ocean bottom than on land (reference Figures 7, 8 and 9).

Some of the more significant features of the seismograms are:

1. The initial P_n arrival is identical but out-of-phase on the pressure and vertical velocity traces until the surface reflection arrives at 0.7 second after the onset; this also holds for the subsequent phases P^*, P_g and S;

2. The phase development is better on the ocean-bottom recording than on land, in contradiction to the results obtained off Santa Catalina Island, California for several underground nuclear blasts reported previously (Semi-Annual Technical Report No. 3, November 1962);

3. The ocean-bottom recording of the event contains more high frequency signal information than does the land recording, and

4. The water arrival or T phase recorded so strongly on the ocean-bottom unit does not appear on land.

In order to compare signal levels and frequency content on the ocean bottom and land, power density spectra were computed over the P - S interval and S arrival. These are shown in Figures 16 and 17 for the P arrival (P - S interval) and S arrival, respectively. The overlays show the average noise power levels on June 29 for both the land and ocean-bottom recordings.

Comparison of the land and ocean-bottom velocity components reveals that the ocean-bottom P signal spectra are relatively enriched in the higher frequencies compared to land. For instance, the vertical ocean-bottom component shows a slightly higher level in the 1 - 2 cps band, but 10 - 18 db more signal power above 2 cps. The horizontals show higher signal power levels at all frequencies, ranging from about 10 db at 1 cps to >30 db at 5 cps. The ocean-bottom horizontal spectra above about 7 cps are corrupted by instrument (or tape) noise as they were obtained from the lo-gain channels.

The pressure P spectra clearly show the filter effect of the water depth. The interference of direct and reflected energy off the water surface causes constructive and destructive interference at frequencies dependent upon the water depth. The tick marks above the curve indicate the frequencies at which constructive interference will occur, $f_n = \frac{1}{\tau}(N - 1/2)$, where τ is the two-way travel time in the water layer. For τ of 0.7 second, the f_n = 0.715, 2.14, 3.56, etc. The observed peaks (and troughs) fit the predicted frequencies well out to 9.3 cps, which suggests very broad band signal energy on the ocean bottom.

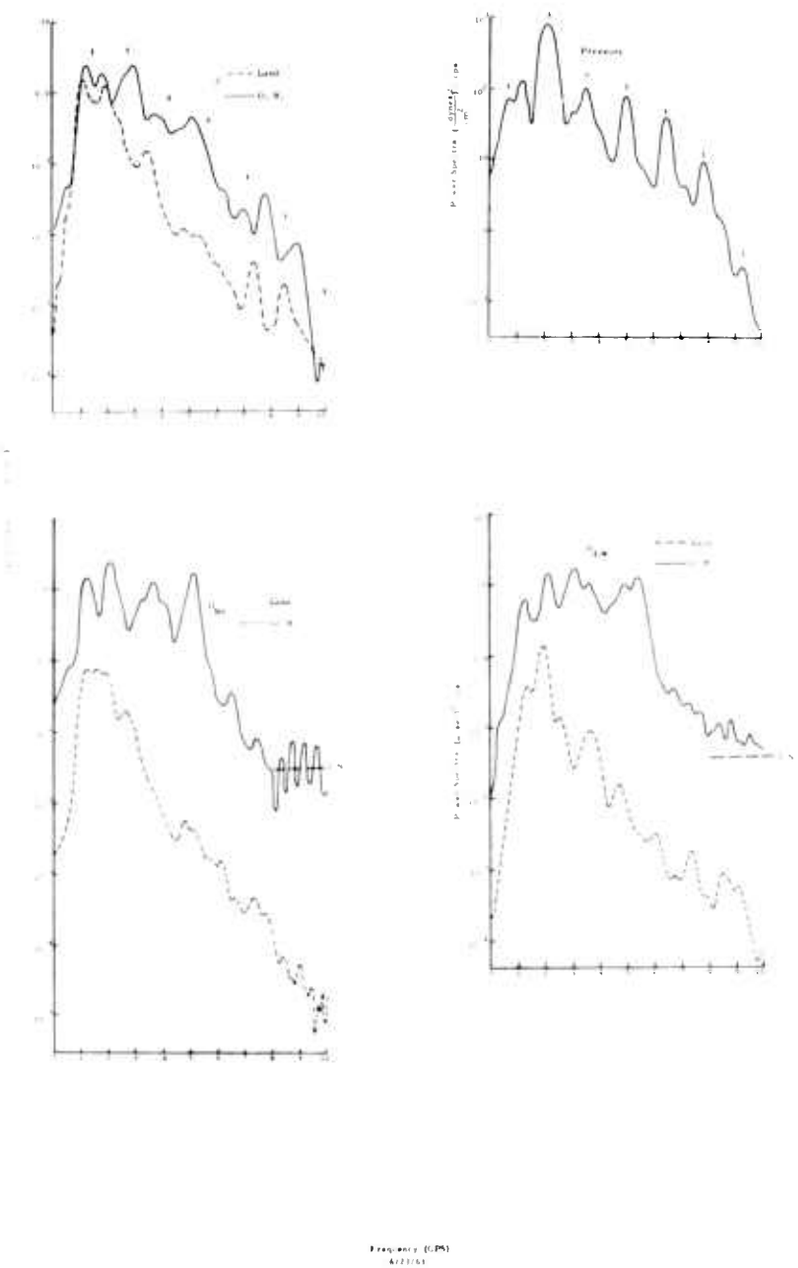

Figure 16. Power Density Spectra, P-S Interval

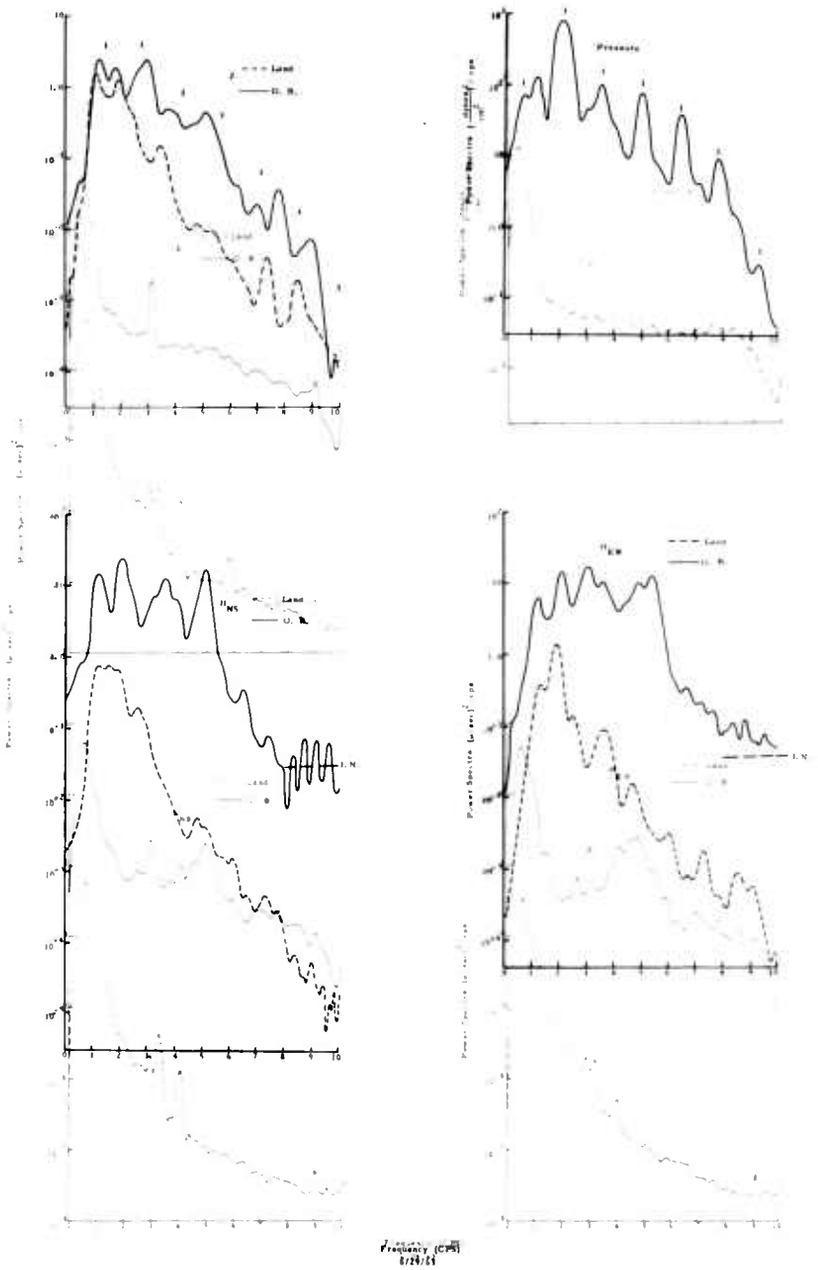

Figure 16. Power Density Spectra, P-S Interval

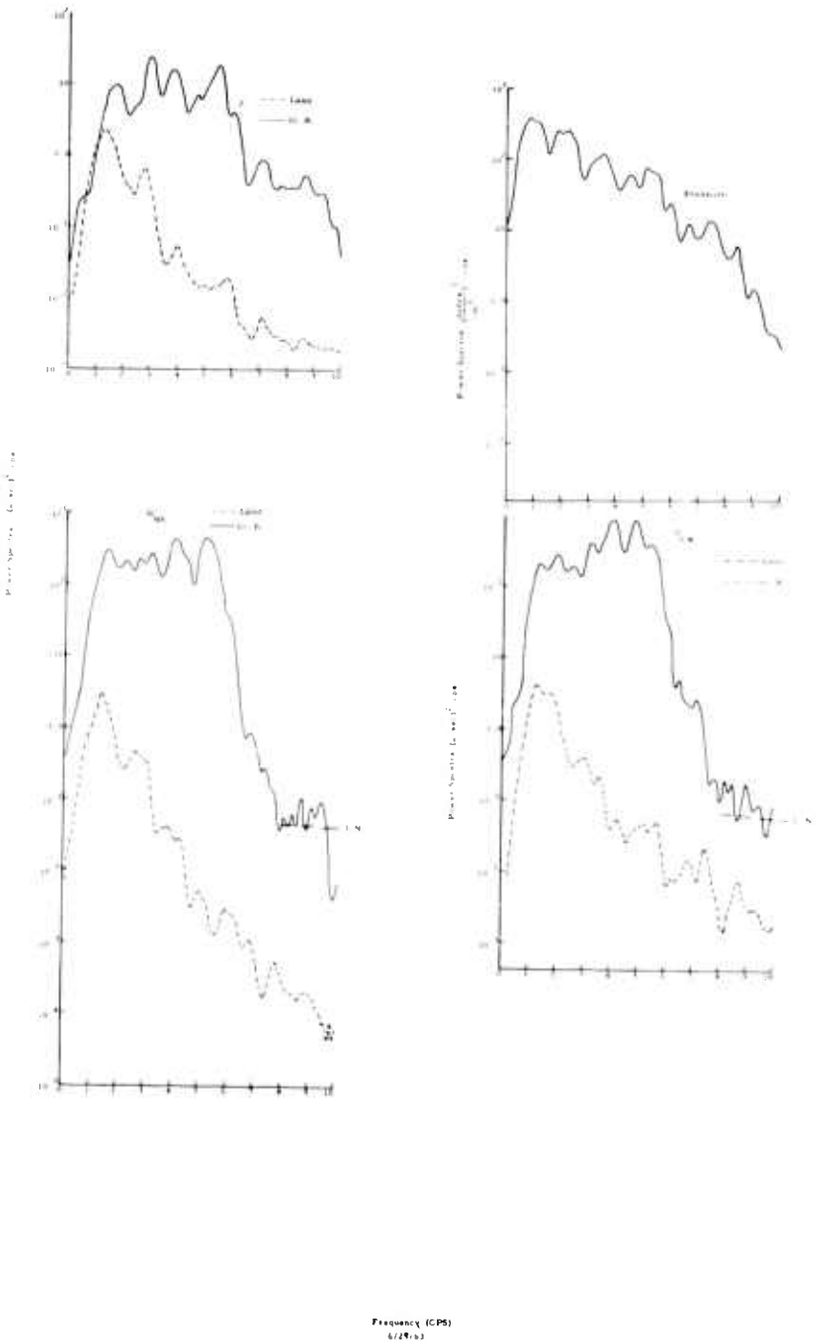

Figure 17. Power Density Spectra, S Interval

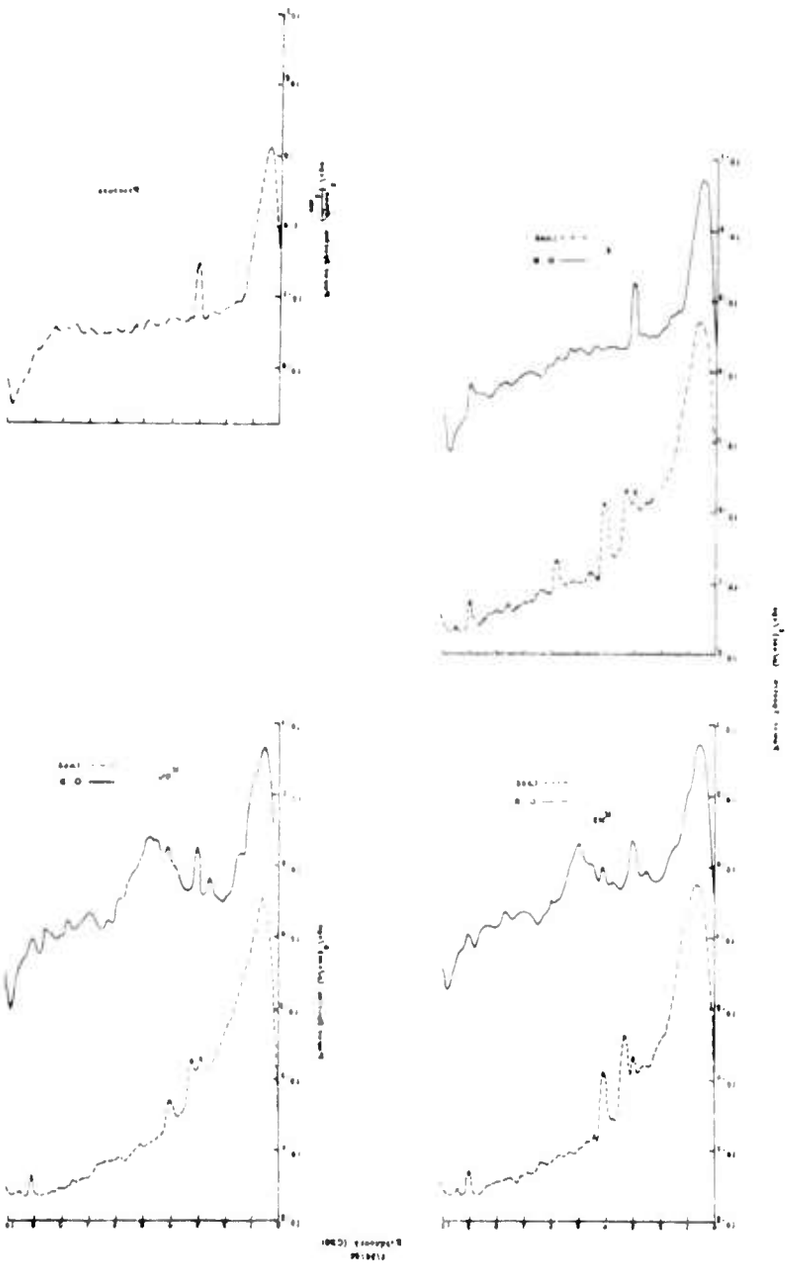

The S power spectra were computed starting at the S phase onset, and extending about 30 seconds thereafter. The early FM clipped portions of the S phase on the land were avoided, and the lo gain vertical channel was used on the ocean-bottom data for the S phase analysis, again due to FM overmodulation of the hi gain channel.

The S phase spectral comparisons afforded in Figure 18 are similar to those of the P phase except that even greater differences in signal level between the ocean bottom and land occur. Again, the higher frequencies are relatively enriched on the ocean bottom.

Locations of the stations and epicenter on June 29 in Figure 12 show that the ranges and azimuths to the ocean-bottom and land sites are 213 km, 250°, and 250 km, 260°, respectively.

The difference in spectral level between the land and ocean bottom cannot be accounted for on the basis of the small range correction. Assuming that a $\frac{1}{R^2}$ amplitude decay with range is appropriate to the various refraction phases, then the ocean-bottom spectrum level should be approximately $\left(\frac{250}{213}\right)^2 = 1.48$ or 3 db higher.

The high frequency attenuation exhibited by the land station relative to the ocean bottom must be related to the additional vertical crustal path of 3400 feet, the difference in elevation between the land and ocean-bottom stations.

The increased signal and noise levels on the ocean bottom relative to a nearby land station are in qualitative agreement with the earlier results reported in Semi-Annual Technical Report No. 3. The relative enrichment of the high frequencies, however, was not evident in the latter.

Pressure-vertical velocity power ratios were also computed for the signal P and S arrivals, and are shown in Figure 18. These illustrate the water depth effect on the pressure and vertical power spectra. The ratio of the power spectra for an upcoming plane wave may be shown to be:

$$\left(\frac{P}{V\rho c}\right)^2 = \frac{1}{(\cos\theta)^2}\left(\frac{\sin \pi f \tau}{\cos \pi f \tau}\right)^2$$

where θ is the angle of refraction of the wave in the water. The predicted peaks agree well with theory for the P arrival, but less so for the S phase. This may be due in part to the presence of other types of arrivals in the S phase, such as locally generated interface waves.

Behavior of the horizontals on the June 29 drop indicates no significant package resonance problem. The latter problem does, however,

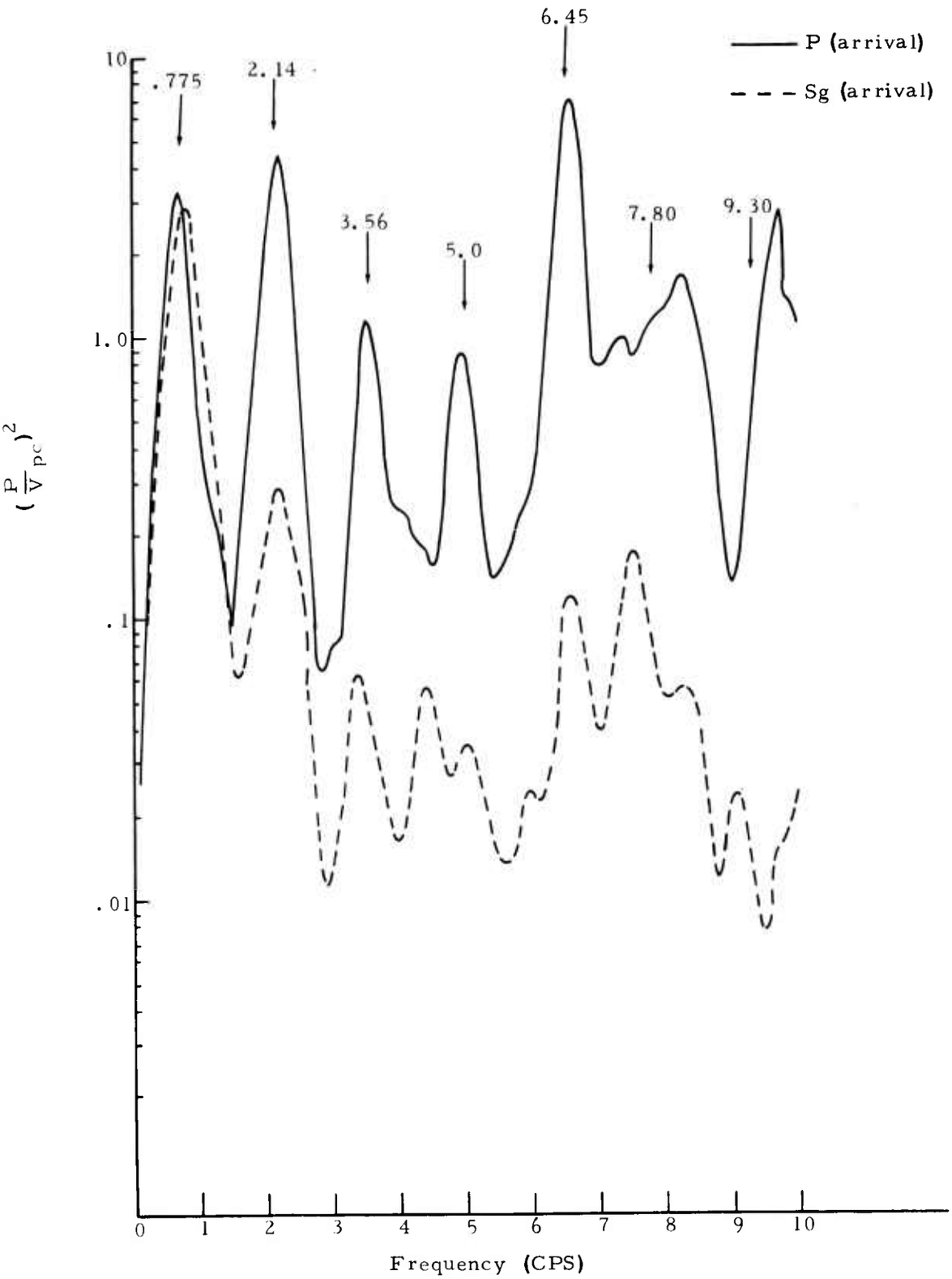

Figure 18. Spectral Comparison - "S" Phase

invalidate much of the horizontal data in subsequent drops, particularly in deeper water. The magnitude of the package resonance phenomenon appears to be very much a function of the specific coupling achieved and bottom conditions in the drop area.

The unidentified signal recorded on July 20, 1963, in 14,820 feet of water, is also shown in the fold-out along with the land recording of the same event. On this drop the ocean-bottom vertical was not operating, thus only the pressure and two horizontals are displayed. The land traces are as before: Benioff vertical, vertical, NS and EW horizontals. A 1.8 cps filter was employed to suppress the prominent microseismic energy.

Pn times indicate the event arrived at the land station first. The first surface reflection can be seen clearly on the pressure trace, which also corroborates the water depth of 14,800 feet. The frequency content on the ocean bottom is again relatively richer in the highs than on land; however, the latter does appear to have a better signal-to-noise ratio in the signal band. The P - S time interval indicates the epicenter is closer to the land station than the ocean bottom.

The ocean-bottom horizontals appear to be somewhat corrupted by package resonance on this drop, particularly the ringing character of the horizontals early in the event. Without the vertical component, it is difficult to establish what portion of the horizontal data is valid. The horizontal-pressure relationships for the later arriving T phase seem quite reasonable in terms of both amplitude and frequency. No spectral analyses of this event were performed because of unknown origin.

Lack of signal events in the California area is somewhat compensated for by the Aleutian data, which yielded some 30 natural events recorded simultaneously on the land station at Adak, and bottom locations north and south of the island arc. Many of these are local events, but they will be analyzed in an effort to extract the significant differences between ocean-bottom and land signal reception.

C. SUMMARY

Analysis completed to date, principally on the California data, indicates that:

1. Ocean-bottom noise power levels are about 20 db greater than at a nearby land station at the microseismic peak;

2. Ocean-bottom and land noise spectra show little variation with time over the samples investigated, and their sources appear to be distributed in azimuth;

3. Ocean-bottom signal levels are higher than on a land station at approximately the same range, with relative enrichment of the high frequencies;

4. The signal phase development for one event is better on the ocean-bottom than on land at approximately the same range.

SEISMIC EVENT

Epicenter: 40.3° N, 126.9 W
Off Coast of Northern California

H = 08:09:27.6 GMT
June 29, 1963
h ≈ 33 Km, Mag. = 4.2
Δ_{OBS} = 213 Km, Az. = 250°
Δ_{Land} = 250 Km, Az. = 260°

OCEAN-BOTTOM SEISMOMETER

Water Depth = 1,750 Ft.

Location:
40°57' N, 124°32' W

- PRESSURE - Hi Gain
- VERTICAL - Hi
- HORIZONTAL U - Lo
- HORIZONTAL L - Lo

LAND SEISMOMETER

Location: 40°41' N, 123°59' W

- BENIOFF VERT. - Lo
- OBS VERTICAL - Lo
- N-S -Lo
- E-W -Lo

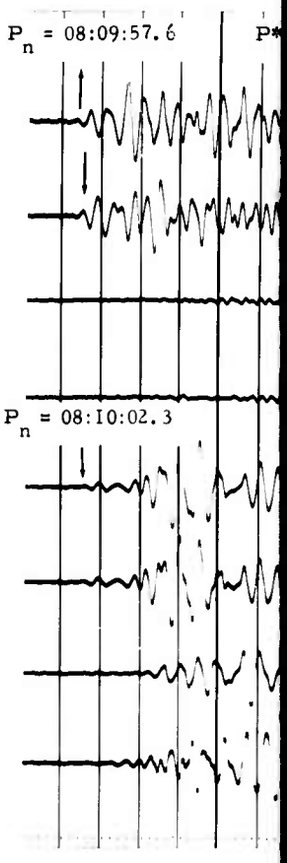

UNLOCATED SEISMIC EVENT

Near Cape Mendocino, California

OCEAN-BOTTOM SEISMOMETER

Water Depth = 14,820 Ft

Location:
40°09' N, 127°35' W

- PRESSURE - Hi Gain
- HORIZONTAL U - Hi
- HORIZONTAL L - Hi

LAND SEISMOMETER

Location:
40°41' N, 123°59' W

- BENIOFF VERTICAL - Lo
- OBS VERTICAL - Lo
- N-S -Lo
- E-W -Lo

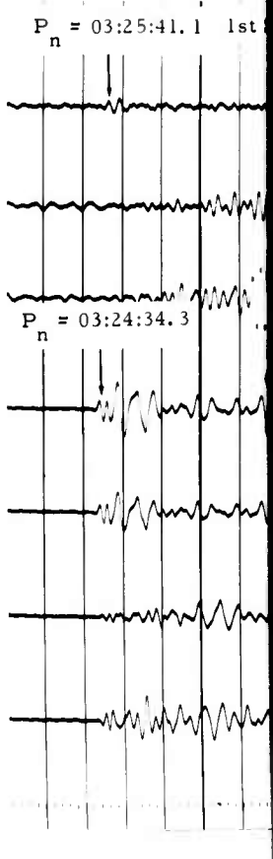

1

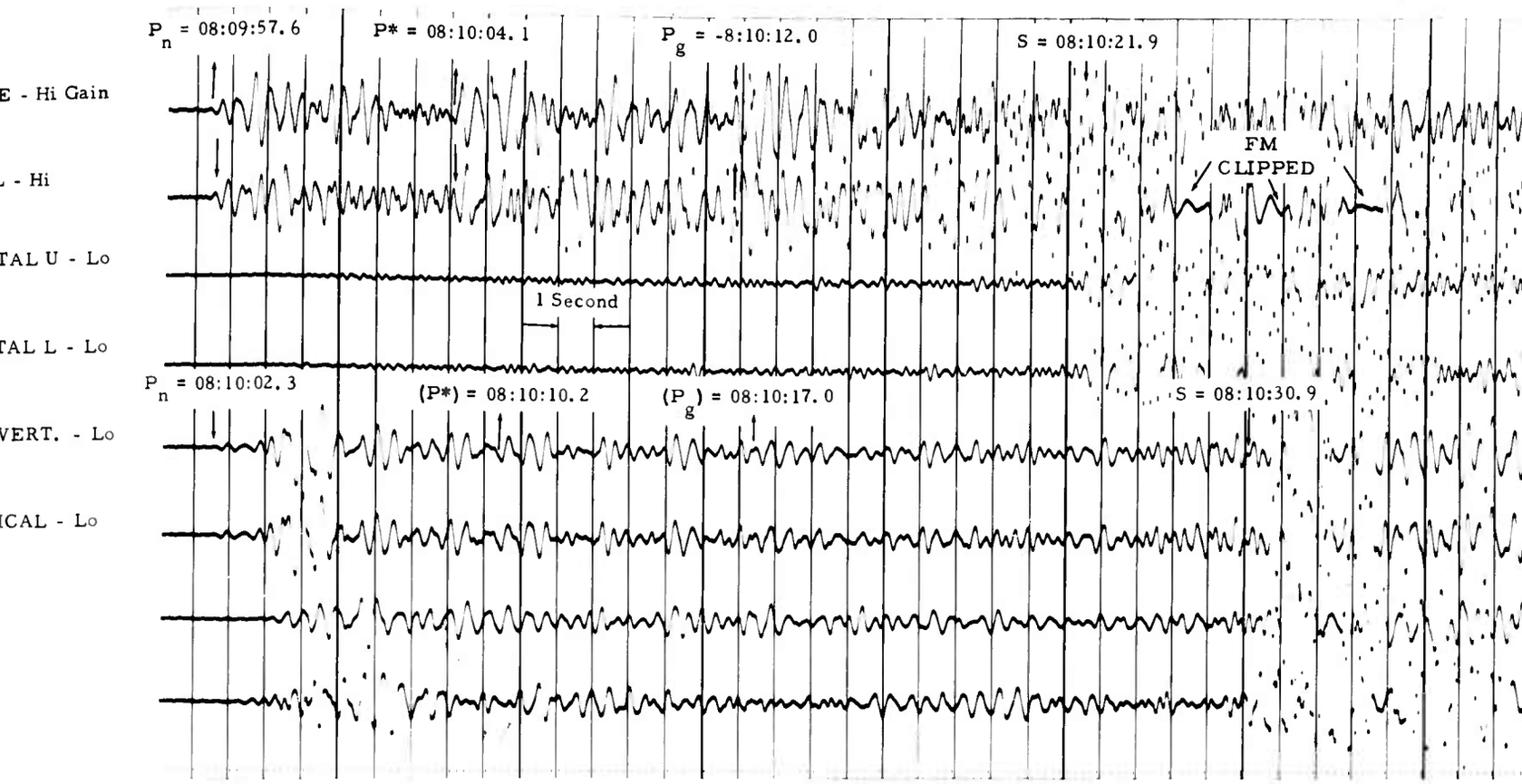
E - Hi Gain
- Hi
TAL U - Lo
TAL L - Lo
VERT. - Lo
ICAL - Lo
P n = 08:09:57.6
P* = 08:10:04.1
P g = -8:10:12.0
S = 08:10:21.9
FM
CLIPPED
1 Second
P n = 08:10:02.3
(P*) = 08:10:10.2
(P g) = 08:10:17.0
S = 08:10:30.9

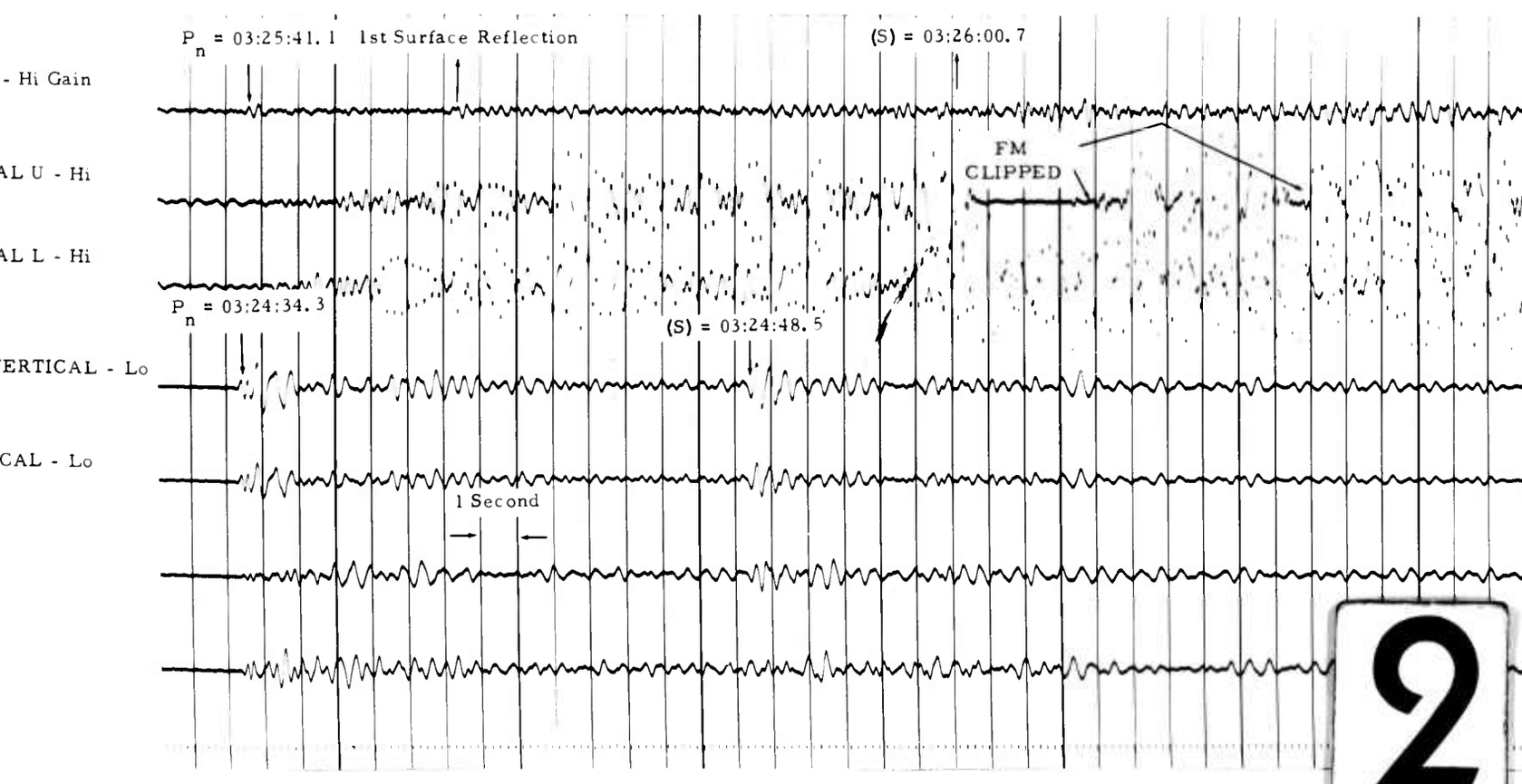
- Hi Gain
AL U - Hi
AL L - Hi
ERTICAL - Lo
CAL - Lo
P n = 03:25:41.1 1st Surface Reflection
(S) = 03:26:00.7
FM
CLIPPED
P n = 03:24:34.3
(S) = 03:24:48.5
1 Second

2

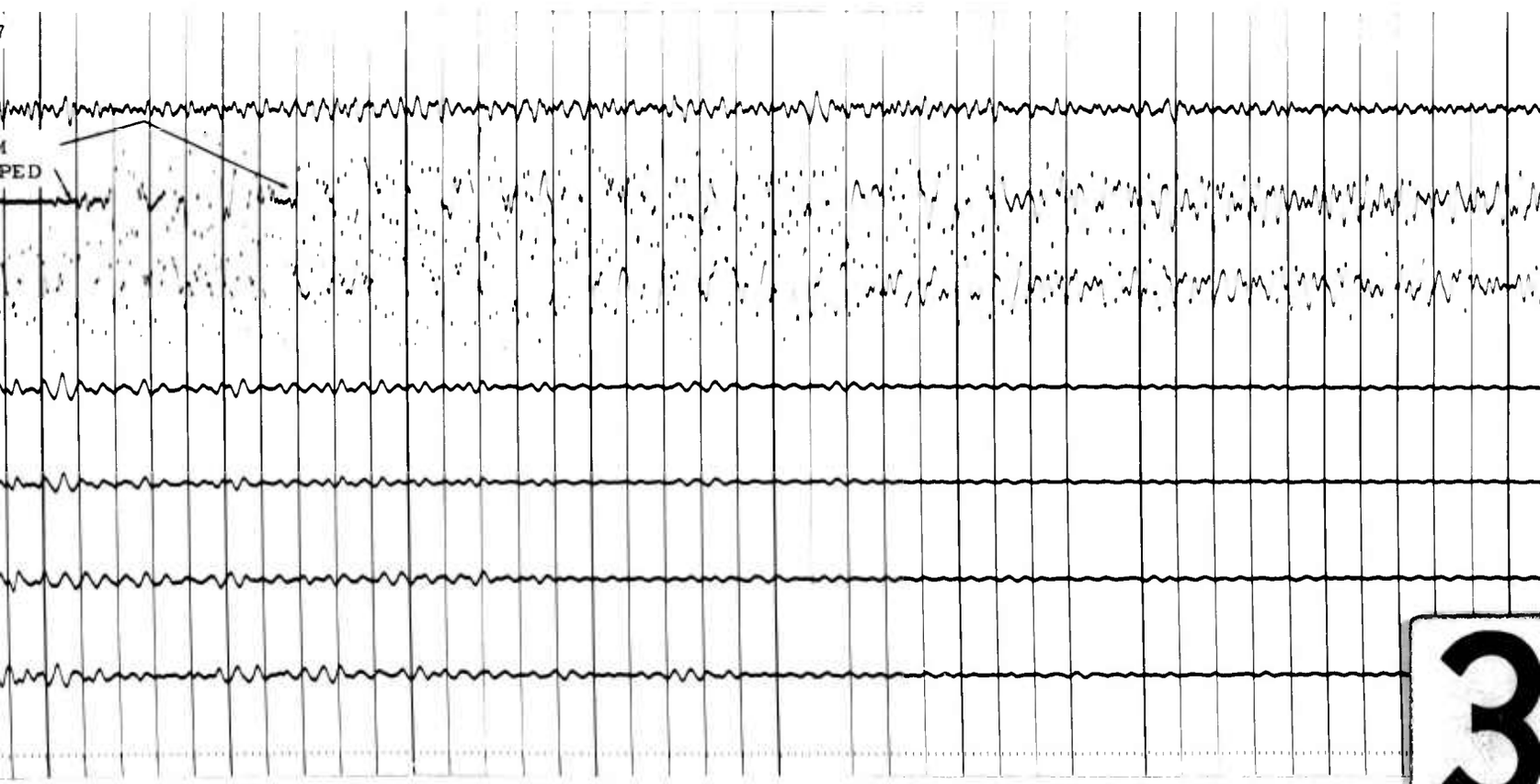

3

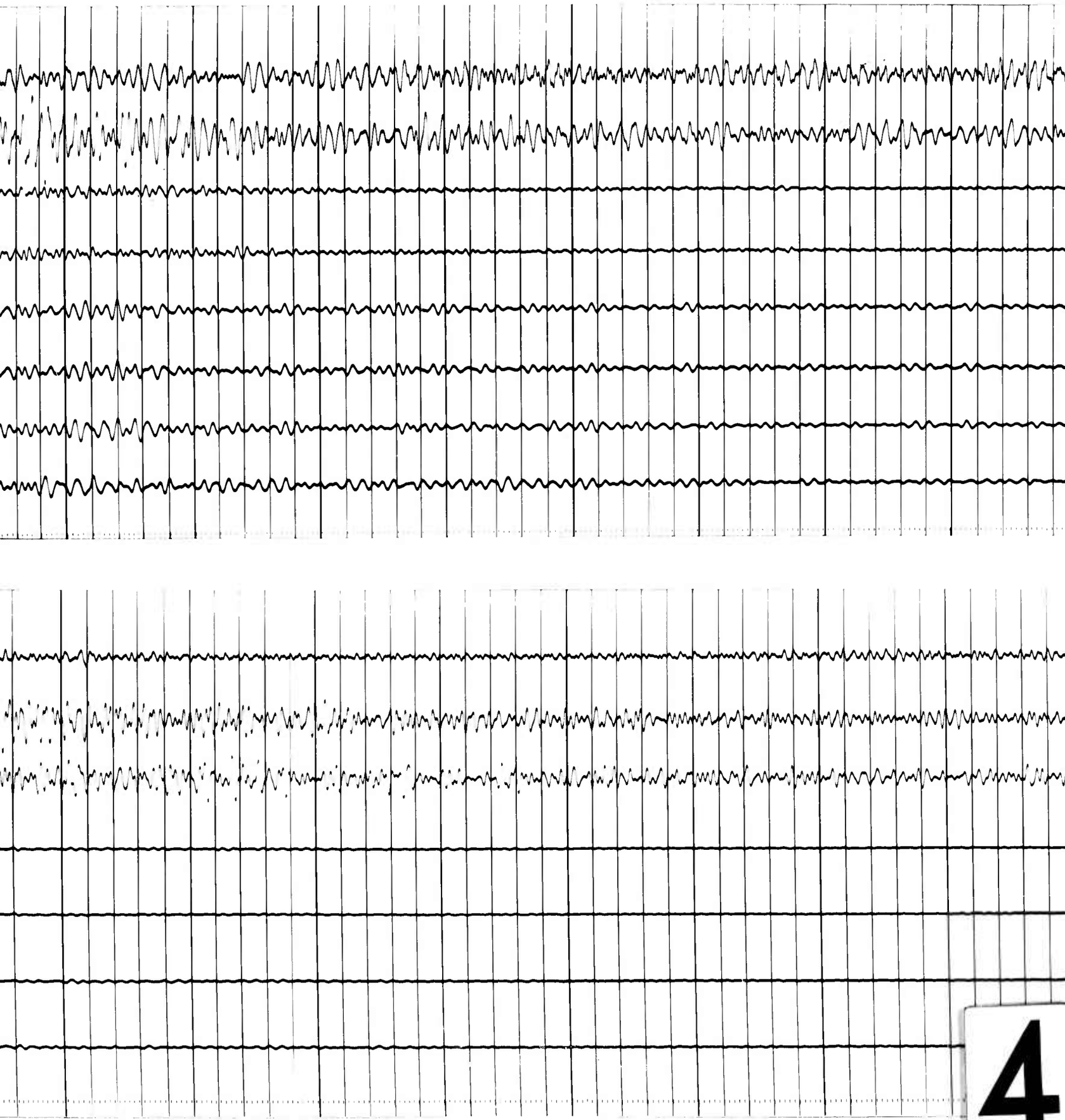

4

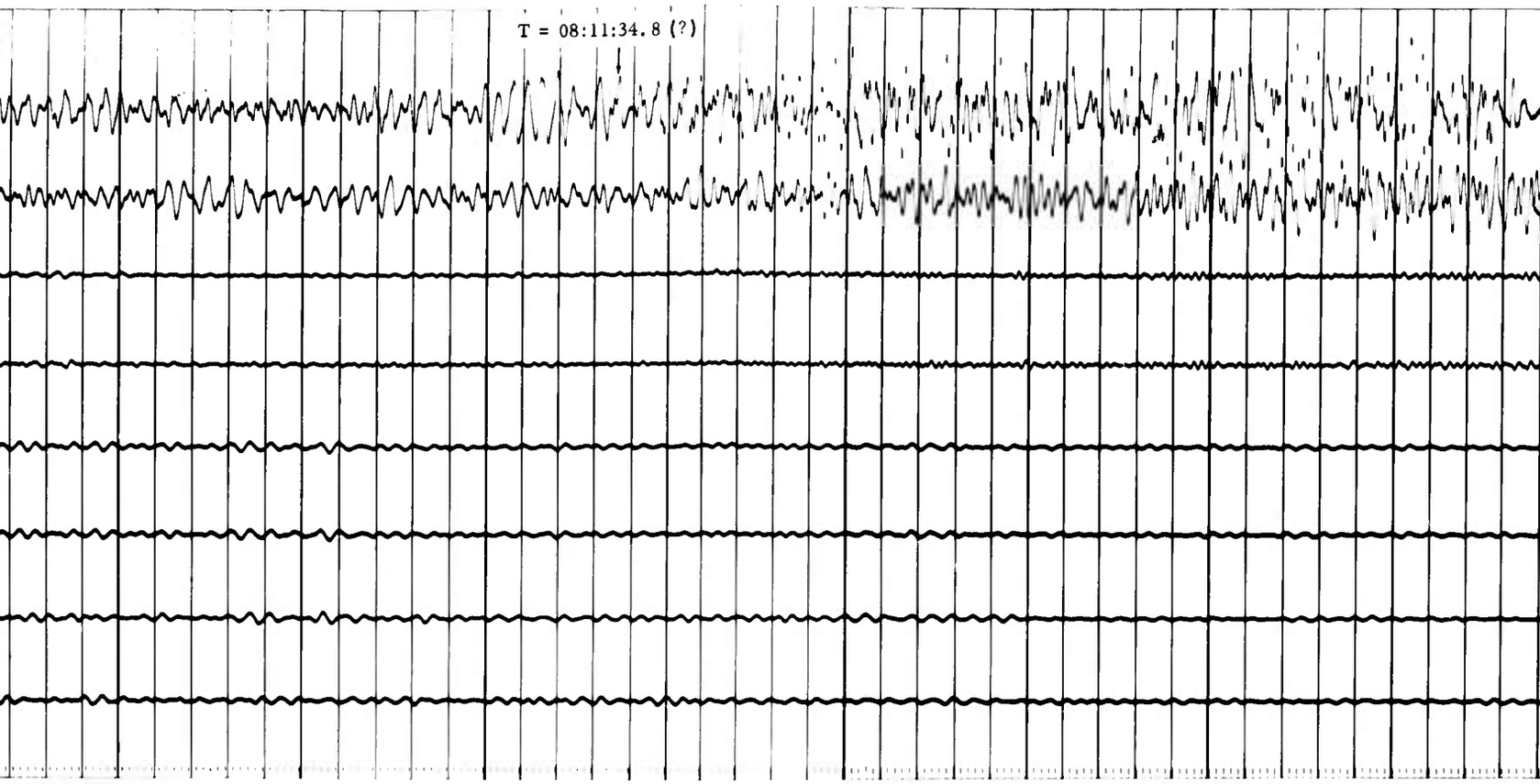
T = 08:11:34.8 (?)

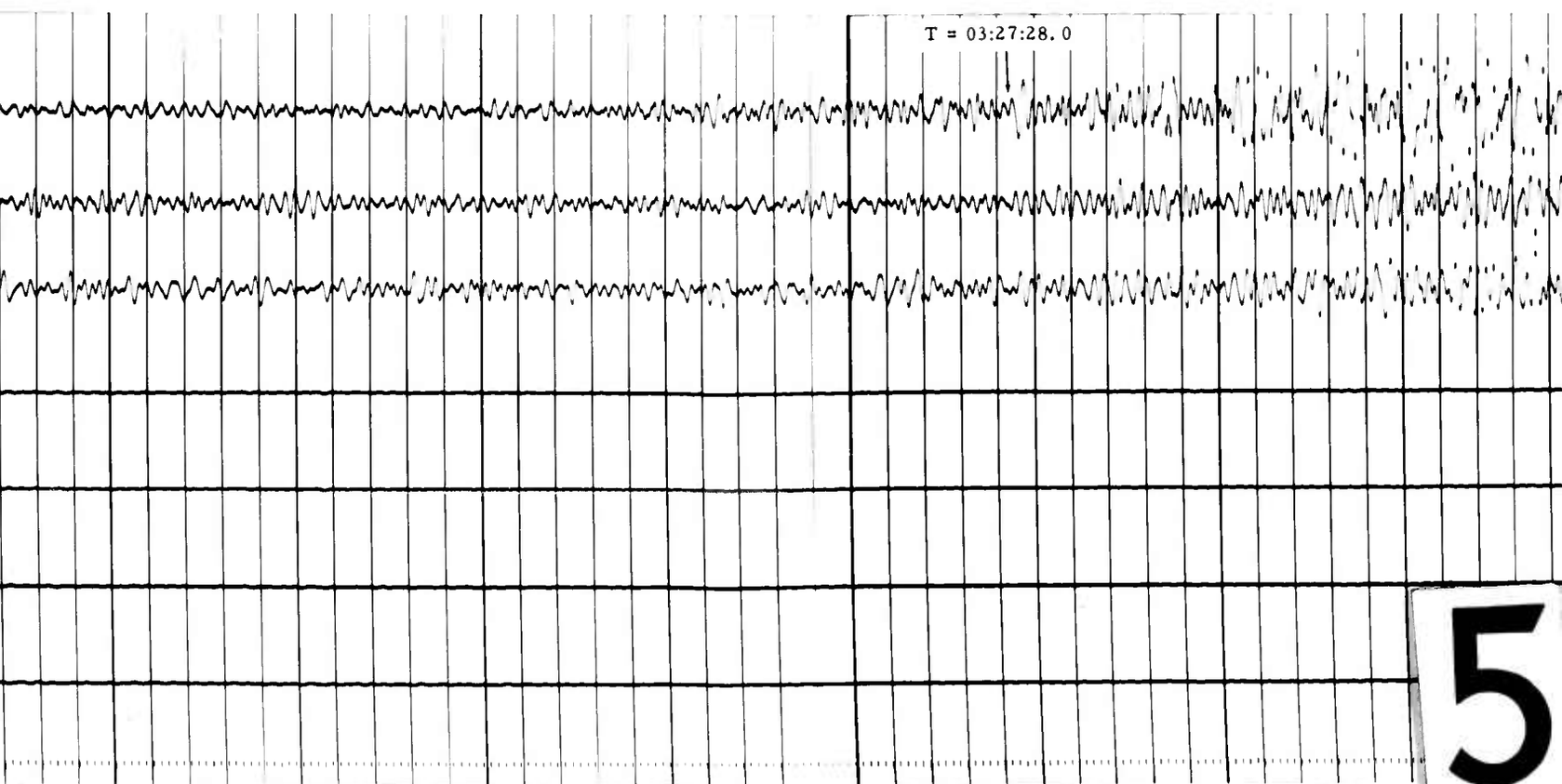
T = 03:27:28.0

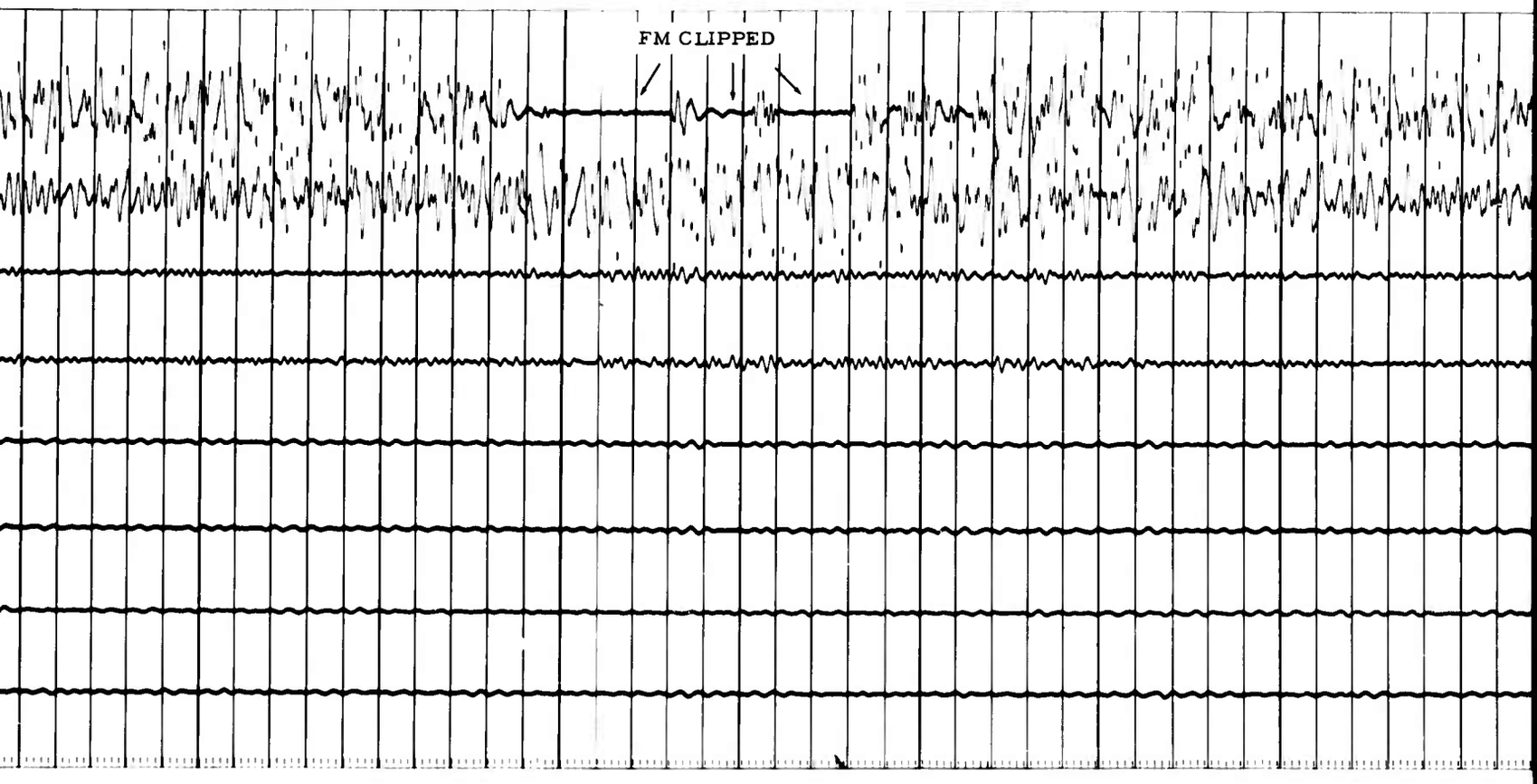

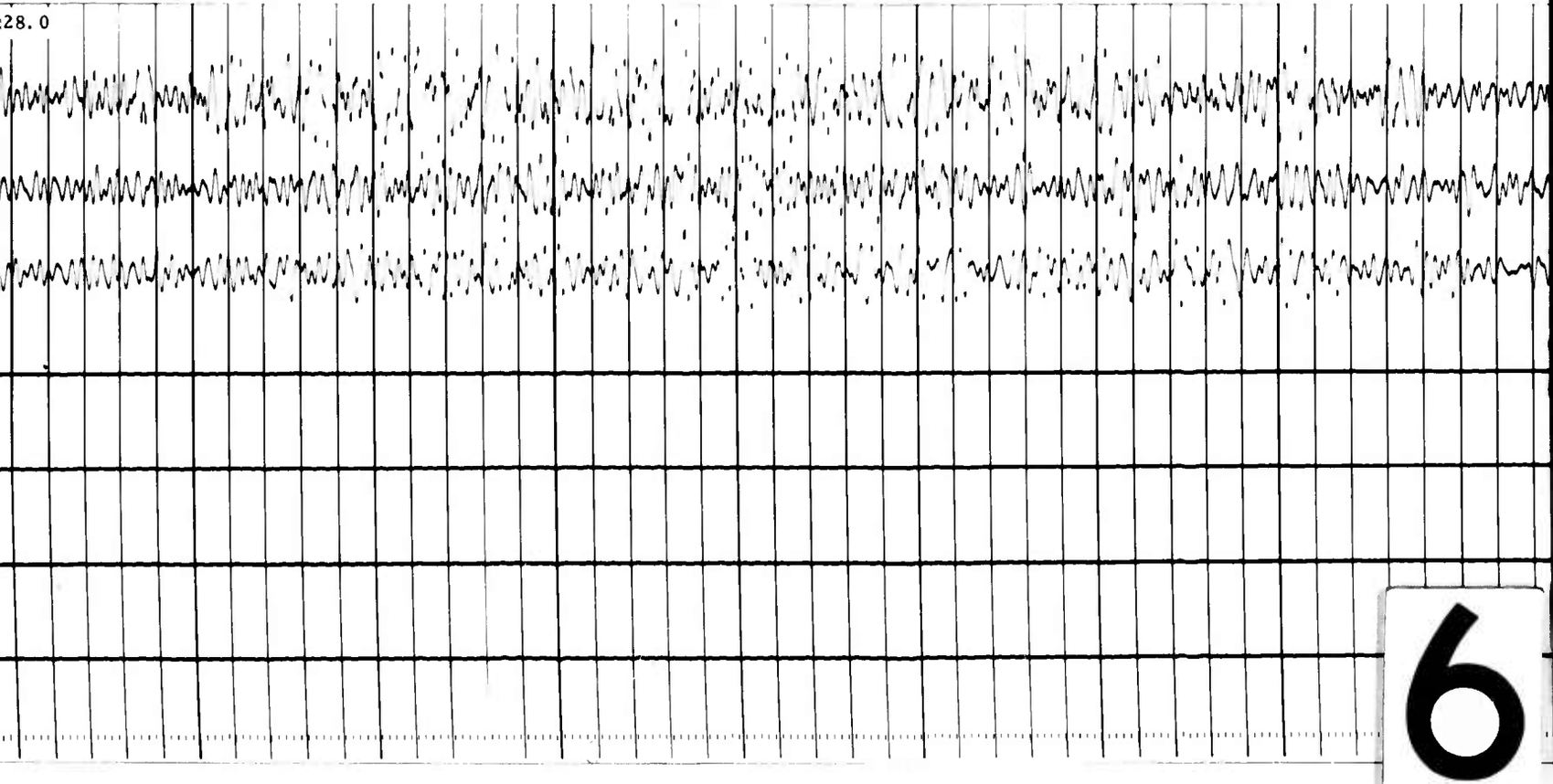

6

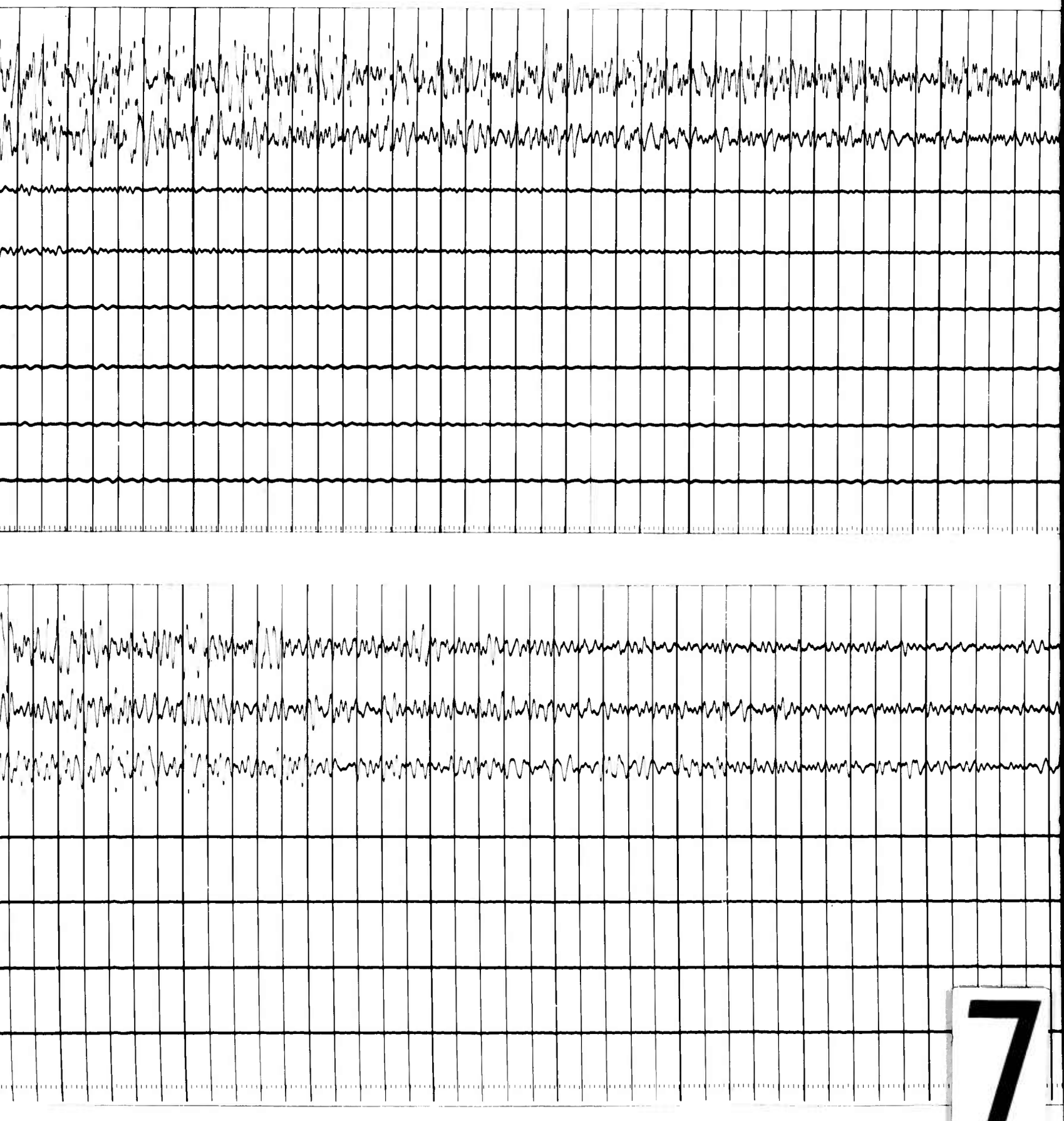

7

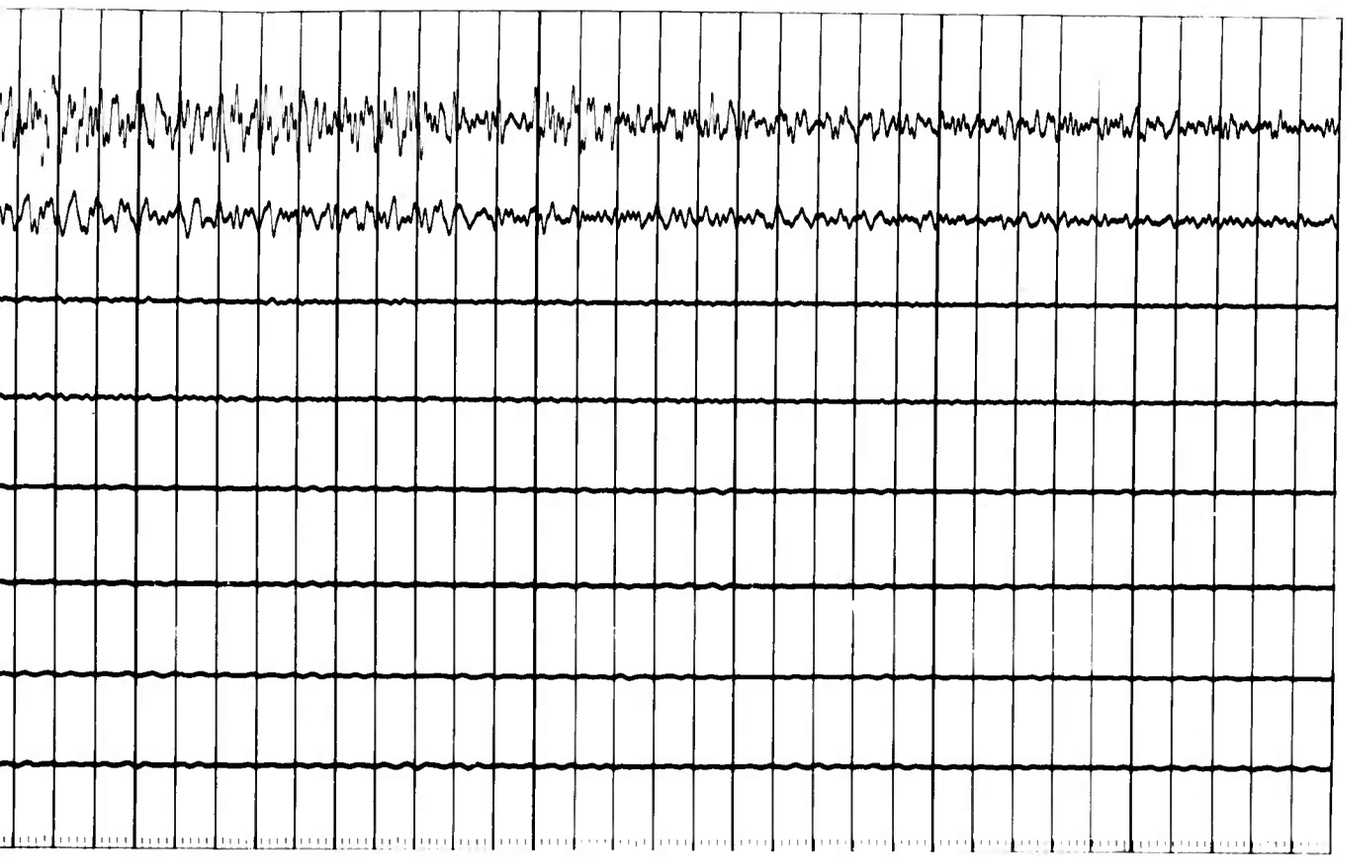

8

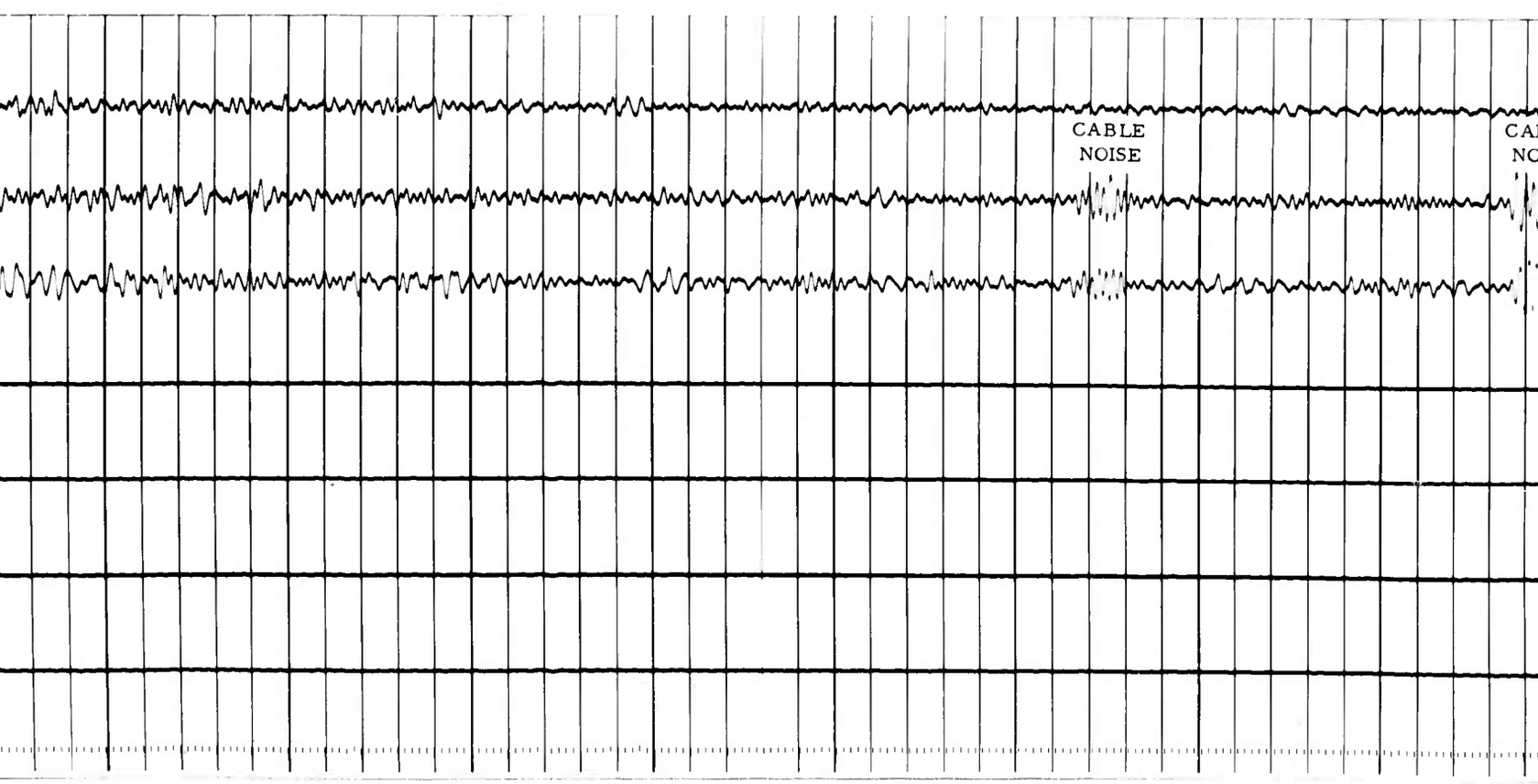

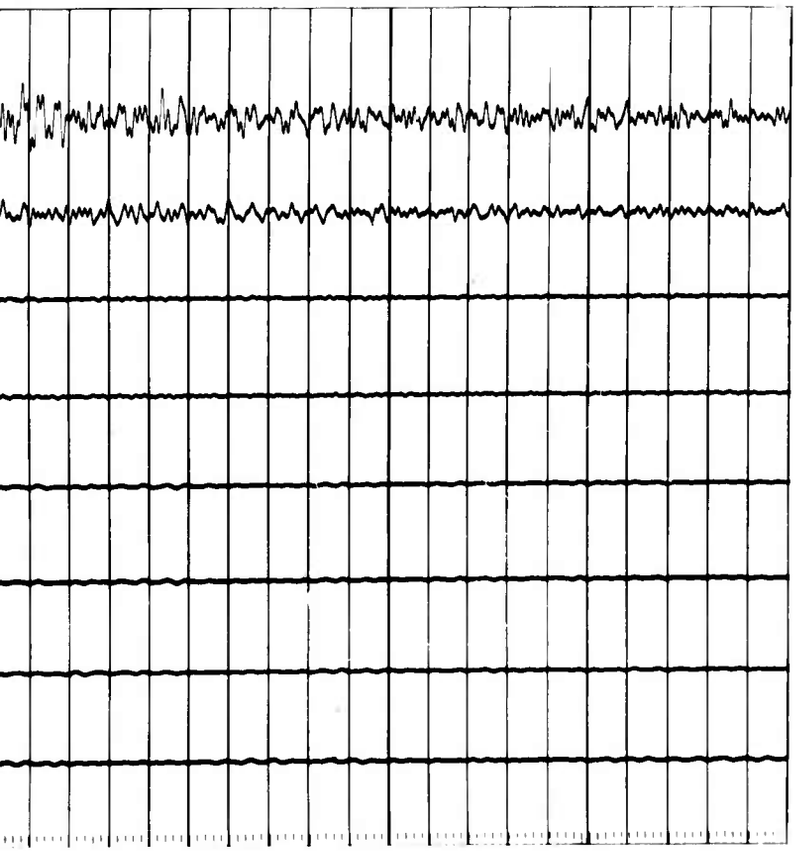

9

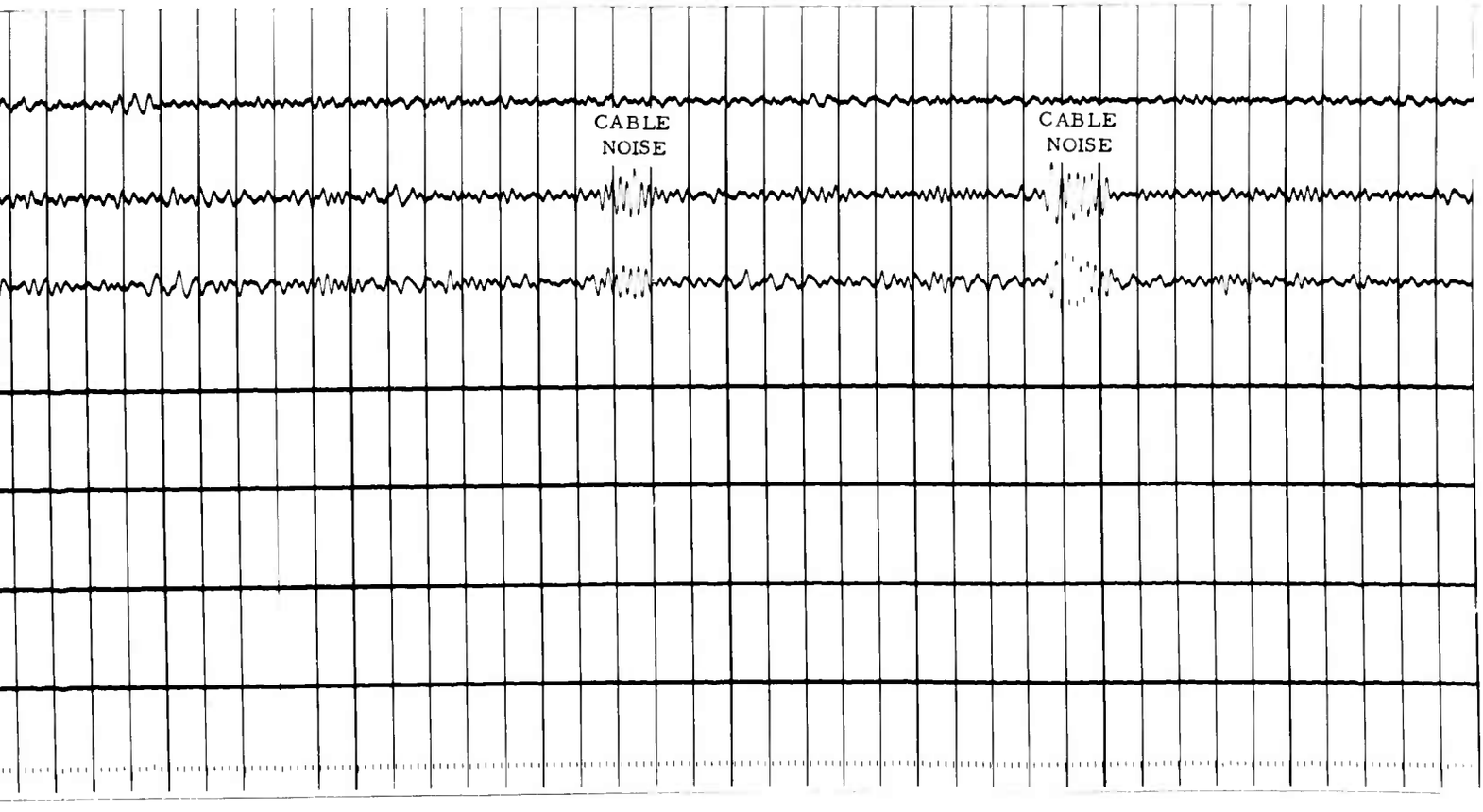

UNCLASSIFIED